This article is a *Plant Cell* Advance Online Publication. The date of its first appearance online is the official date of publication. The article has been edited and the authors have corrected proofs, but minor changes could be made before the final version is published. Posting this version online reduces the time to publication by several weeks.

Transposase-Derived Proteins FHY3/FAR1 Interact with PHYTOCHROME-INTERACTING FACTOR1 to Regulate Chlorophyll Biosynthesis by Modulating *HEMB1* during Deetiolation in *Arabidopsis* [W]

Weijiang Tang,[a,1] Wanqing Wang,[a,b,1] Dongqin Chen,[a] Qiang Ji,[a,b] Yanjun Jing,[a] Haiyang Wang,[c,d] and Rongcheng Lin[a,2]

[a] Key Laboratory of Photobiology, Institute of Botany, Chinese Academy of Sciences, Beijing 100093, China
[b] Graduate School of the Chinese Academy of Sciences, Beijing 100049, China
[c] College of Life Sciences, Capital Normal University, Beijing 100048, China
[d] Department of Molecular, Cellular, and Developmental Biology, Yale University, New Haven, Connecticut 06520

Successful chlorophyll biosynthesis during initial light exposure is critical for plant survival and growth, as excess accumulation of chlorophyll precursors in darkness can cause photooxidative damage to cells. Therefore, efficient mechanisms have evolved to precisely regulate chlorophyll biosynthesis in plants. Here, we identify FAR-RED ELONGATED HYPOCOTYL3 (FHY3) and FAR-RED IMPAIRED RESPONSE1 (FAR1), two transposase-derived transcription factors, as positive regulators of chlorophyll biosynthesis in *Arabidopsis thaliana*. We show that null mutations in *FHY3* and *FAR1* cause reduced protochlorophyllide (a precursor of chlorophyll) levels in darkness and less photobleaching in the light. We find that FHY3 directly binds to the promoter and activates expression of *HEMB1*, which encodes 5-aminolevulinic acid dehydratase in the chlorophyll biosynthetic pathway. We reveal that PHYTOCHROME-INTERACTING FACTOR1 physically interacts with the DNA binding domain of FHY3, thereby partly repressing FHY3/FAR1-activated *HEMB1* expression. Strikingly, FHY3 expression is upregulated by white light. In addition, our genetic data indicate that overexpression, severe reduction, or lack of *HEMB1* impairs plant growth and development. Together, our findings reveal a crucial role of FHY3/FAR1 in regulating chlorophyll biosynthesis, thus uncovering a new layer of regulation by which light promotes plant dark–light transition in early seedling development.

INTRODUCTION

As sessile organisms, plants respond to the surrounding environments by shaping their growth and development. Light is one of the major environmental signals that influences plants throughout their life cycle, from seed germination to flowering. Under the soil, germinating seedlings undergo etiolation (also called skotomorphogenesis) with long hypocotyls and closed cotyledons lacking chlorophyll and functional chloroplasts. Upon emerging from the soil and reaching light, the etiolated seedlings undergo deetiolation (also termed photomorphogenesis), including cotyledon opening, chlorophyll biosynthesis, the development of chloroplasts, and subsequently autotrophic growth (Von Arnim and Deng, 1996, Casal et al., 2004).

Phytochrome and cryptochrome photoreceptors are responsible for perceiving and transducing light signals to regulate distinct photomorphogenic responses. In *Arabidopsis thaliana*, phytochrome A (phyA) to phyE form a small protein family that predominantly regulates various responses to red and far-red light, whereas the cryptochromes (cry1 and cry2) absorb the blue/UV-A light (Whitelam et al., 1993; Neff et al., 2000; Lin 2002). phyA is the primary photoreceptor for mediating far-red light signaling. FAR-RED ELONGATED HYPOCOTYL3 (FHY3) and FAR-RED-IMPAIRED RESPONSE1 (FAR1) are homologous proteins that function as positive regulators and act early in phyA signaling (Hudson et al., 1999; Wang and Deng, 2002; Wang et al., 2002). They work together to modulate phyA nuclear accumulation and phyA responses through directly activating gene expression of a pair of downstream targets, *FHY1* and *FHY1-LIKE* (Lin et al., 2007, 2008). Studies also showed that FHY3 and FAR1 integrate light signals into the circadian clock and modulate chloroplast division by directly upregulating expression of *EARLY FLOWERING4* and *ACCUMULATION AND REPLICATION OF CHLOROPLASTS5* (*ARC5*), respectively (Allen et al., 2006; Li et al., 2011; Ouyang, et al., 2011). We and others previously documented that FHY3 and FAR1 define a type of transcription factors that were derived from ancient transposases during evolution and may play diverse roles (Hudson et al., 2003; Lin et al., 2007). A recent study found that FHY3 has more than a thousand putative direct targets in *Arabidopsis* (Ouyang et al., 2011), implicating it as having broad functions in plant growth and development, most of which, however, are unknown.

[1] These authors contributed equally to this work.
[2] Address correspondence to rclin@ibcas.ac.cn.
The author responsible for distribution of materials integral to the findings presented in this article in accordance with the policy described in the Instructions for Authors (www.plantcell.org) is: Rongcheng Lin (rclin@ibcas.ac.cn).
[W] Online version contains Web-only data.
www.plantcell.org/cgi/doi/10.1105/tpc.112.097022

Chlorophyll formation is a hallmark of the photomorphogenic response, and chlorophylls serve as the major pigments in photosynthesis by harvesting light energy and driving electron transfer. Chlorophyll metabolism has been extensively studied with various organisms biochemically and genetically (Eckhardt et al., 2004; Tanaka and Tanaka, 2006, 2007). Chlorophyll biosynthesis shares early steps from the first committed precursor 5-aminolevulinic acid (ALA) to protoporphyrin IX with that of heme, siroheme, and phytochromobilin in the tetrapyrrole biosynthetic pathway (Battersby, 2000; Tanaka and Tanaka, 2007; Mochizuki et al., 2010). Two molecules of ALA are then condensed to form a pyrrole molecule, porphobilinogen (PBG), by ALA dehydratase (ALAD). After sequential enzymatic conversions, the pathway is divided by metal chelation reactions of protoporphyrin IX, thereby directing the formation of the end products chlorophyll and heme (Tanaka and Tanaka, 2007). In darkness, the chlorophyll biosynthetic branch is blocked at the intermediate protochlorophyllide (Pchlide) because the conversion of Pchlide to chlorophyllide is catalyzed by the light-dependent enzyme NADPH:protochlorophyllide oxidoreductase (POR) in plants (Runge et al., 1996; Su et al., 2001; Heyes and Hunter, 2005; Solymosi and Schoefs, 2010). However, the accumulation of excess free Pchlide and/or other pyrrole intermediates in darkness may produce reactive oxygen species (ROS) upon light irradiation and thereby cause cotyledon photobleaching or even cell death (Reinbothe et al., 1996; op den Camp et al., 2003; Wagner et al., 2004; Buhr et al., 2008). Therefore, chlorophyll biosynthesis is critical for plant survival and must be properly regulated, particularly during the switch from skotomorphogenesis to photomorphogenesis. Plants have evolved efficient mechanisms to regulate Pchlide content precisely in the dark.

Accumulating evidence shows that the biosynthetic pathway is primarily subject to transcriptional and posttranslational regulation (Tanaka and Tanaka, 2007; Mochizuki et al., 2010). ALA formation is viewed as a control point for regulation of chlorophyll supply. FLUORESCENT (FLU) was identified as an important regulatory protein that represses ALA synthesis by binding and thereby inhibiting the activity of glutamyl-tRNA reductase (GluTR) encoded by *HEMA1* (Meskauskiene et al., 2001; Goslings et al., 2004). GluTRBP is the second GluTR binding protein that mediates spatial separation of ALA into heme biosynthesis (Czarnecki et al., 2011). Another regulator, GENOMES UNCOUPLED4 (GUN4), interacts with Mg-chelatase and stimulates its activity by facilitating substrate binding and/or product release (Larkin et al., 2003; Adhikari et al., 2011). These proteins are crucial for plant survival as a *flu* loss-of-function mutation is lethal during deetiolation or when plants are grown in light-dark cycles, whereas lack of *GluTRBP* is lethal and absence of *GUN4* causes a complete absence of chlorophyll (Meskauskiene et al., 2001; Peter and Grimm, 2009).

Recently, several transcription factors have been found to play important roles in regulating chlorophyll biosynthesis during seedling deetiolation. The PHYTOCHROME-INTERACTING FACTORs (including PIF1, PIF3, PIF4, and PIF5) are a subset of the basic helix-loop-helix family of transcription factors and act as negative regulators of diverse phytochrome-mediated signaling responses (Leivar and Quail, 2011). In darkness, *pif* mutants display constitutive photomorphogenic phenotypes and overaccumulate Pchlide. Their etiolated cotyledons are severely photobleached after subsequent light illumination (Huq et al., 2004; Monte et al., 2004; Moon et al., 2008; Shin et al., 2009; Stephenson et al., 2009). It is believed that PIFs are negative regulators of chlorophyll biosynthesis in the dark and that light derepresses this response by triggering the proteasome-mediated degradation of PIFs (Al-Sady et al., 2006; Leivar et al., 2009; Shin et al., 2009; Shen et al., 2005). PIF1 directly regulates chlorophyll biosynthesis by binding the promoter of *PORC* and activating its gene expression (Moon et al., 2008), whereas PIF3 indirectly regulates a number of biosynthetic genes, such as *HEMA1* and *GUN5* (Shin et al., 2009; Stephenson et al., 2009). It was also shown that ETHYLENE INSENSITIVE3 (EIN3) and its homolog EIN3-LIKE1 cooperate with PIF1 to inhibit Pchlide accumulation. EIN3 is able to upregulate *PORA* and *PORB* gene expression directly. Consequently, their loss-of-function mutants accumulate excess Pchlide in etiolated seedlings and became photobleached when transferred to light (Zhong et al., 2009). A recent study demonstrated that DELLA proteins upregulate *POR* expression and limit the accumulation of ROS and photooxidative damage in PIF-dependent and -independent manners during seedling deetiolation (Cheminant et al., 2011). These studies together reveal that *POR* is an important target for transcriptional regulation in chlorophyll biosynthesis, consistent with its function in conversion of Pchlide into chlorophyllide during seedling deetiolation. However, the mechanism for direct regulation of Pchlide levels is still not understood.

In this study, we provide genetic, molecular and biochemical evidence to demonstrate that FHY3 and FAR1 redundantly promote chlorophyll biosynthesis by directly binding to and activating the expression of *HEMB1*, which encodes ALAD, with FHY3 playing a predominant role. We show that FHY3 physically interacts with the negative transcription regulator PIF1 to coordinate Pchlide synthesis and seedling greening. Furthermore, *FHY3* expression is upregulated by white light during deetiolation. Our finding highlights FHY3 and FAR1 as positive and key transcription factors in directly regulating chlorophyll biosynthesis for seedling survival and provides insight into the functional divergence of these transposase-derived transcription factors in plants during evolution.

RESULTS

FHY3/FAR1 Promote Pchlide Accumulation in Etiolated Seedlings

A previous transcriptome analysis of *Arabidopsis* seedlings indicates that most of the genes involved in tetrapyrrole biosynthesis are highly responsive to light (Matsumoto et al., 2004). We speculated that there might exist a direct positive regulator(s) of Pchlide biosynthesis in etiolated seedlings. To this end, we tested some known transcription factors that have been demonstrated to be key components in the light signaling pathway (Jiao et al., 2007). Five-day-old etiolated seedlings of various mutants and the wild type were incubated with acetone overnight, and Pchlide levels were compared by scanning the

fluorescence emission in a fluorescence spectrophotometer (Huq et al., 2004). Consistent with previous studies, *pif1* and *pif3* mutants accumulated extremely high levels of Pchlide compared with the wild type (Huq et al., 2004; Moon et al., 2008; Shin et al., 2009; see Supplemental Figure 1 online). The *elongated hypocotyl5 homolog* (*hyh*), *long hypocotyl in far-red1* (*hfr1*), and *long after far-red light1* (*laf1*) mutants also had slight increased amounts of Pchlide. By contrast, the Pchlide content was decreased in the *fhy3* mutant and was slightly reduced in the *far1* and *hy5* mutants compared with their corresponding wild-type seedlings (Figure 1A; see Supplemental Figure 1 online), suggesting that FHY3, FAR1, and HY5 may play positive roles in regulating chlorophyll biosynthesis in the dark. In this study, we focused on the roles of FHY3 and FAR1. We further found that the *fhy3 far1* double mutant had even less Pchlide accumulation than their single mutant parents (Figure 1A), demonstrating a redundant function between these two proteins, with FHY3 playing a predominant role. In the following experiments, the function and mechanism of FHY3 will be investigated in more detail. To confirm whether low Phclide in the *fhy3-4* mutant is caused by the disruption of FHY3 protein, a *FHY3p*:*FHY3* transgene in which the *FHY3* open reading frame (ORF) is under the control of its own promoter was introduced into *fhy3-4* (Lin et al., 2008). The transgene was found to complement the *fhy3-4* mutant phenotype (Figure 1B). In addition, dexamethasone (DEX; 1 μM) treatment greatly restored the Pchlide level of *fhy3-4*/*FHY3P*:*FHY3-GR* transgenic plants (Lin et al., 2007) compared with mock-treated plants (Figure 1C), suggesting that nuclear targeting of FHY3 is required for its function. These results reveal that FHY3 and FAR1 promote Pchlide accumulation and likely function as positive regulators of chlorophyll biosynthesis in the dark.

Because the tetrapyrrole biosynthetic pathway separates into two different branches to produce heme and chlorophyll, we then tested if the heme branch was also affected by the *fhy3* and *far1* mutations. Noncovalently bound heme was extracted from 5-d-old etiolated seedlings and measured spectrophotometrically. However, no difference in heme production was observed between *fhy3 far1*, *fhy3*, and *far1* mutants and the wild type (see Supplemental Figure 2 online).

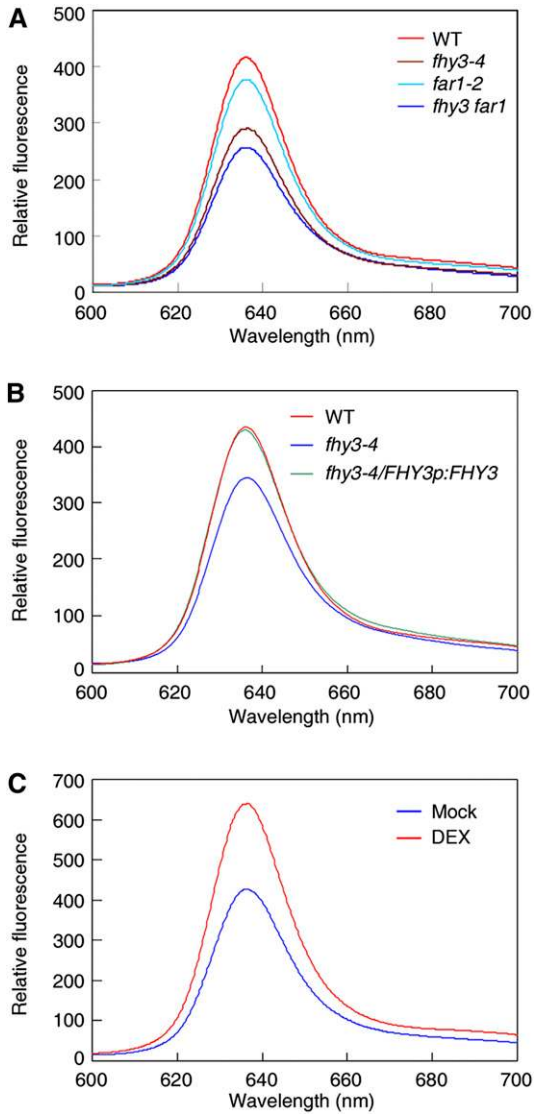

Figure 1. FHY3/FAR1 Promote Pchlide Accumulation in Darkness.

(A) Pchlide level of 5-d-old dark-grown wild-type (WT) and various mutant seedlings.

(B) Pchlide level of 5-d-old dark-grown *fhy3-4*/*FHY3p*:*FHY3* transgenic line with *fhy3-4* mutant and the wild type.

(C) Pchlide level of *fhy3-4*/*FHY3p*:*FHY3-GR* transgenic seedlings grown in the dark on MS medium with or without 1 μM DEX for 4 d.

Loss of FHY3/FAR1 Enhances Seedling Greening during Deetiolation

Next, we investigated how *fhy3* and *far1* mutations might influence the seedling deetiolation process. Etiolated seedlings grown in extended periods of darkness were illuminated with normal intensity white light (150 μmol m^{-2} s^{-1}), and the percentage of green cotyledons (greening rate) was calculated after an additional 2 d. We found that the greening rate of *fhy3-4* was much higher than that of the wild type after 4 d or longer of dark treatment. The *far1-2* mutant showed a slightly increased greening rate compared with the wild type when grown in the dark for 6 d. Remarkably, the *fhy3 far1* double mutant possessed strong greening ability, with a greening rate of nearly 75% even after 7 d of darkness (Figures 2A and 2B). Then we tested the greening process by transferring seedlings to various light intensities after 5 d of darkness. There were no distinguishable differences under low light conditions (<80 μmol m^{-2} s^{-1}). However, when seedlings were transferred to light intensities of 150 μmol m^{-2} s^{-1} or higher, the greening rates of *fhy3-4* and especially *fhy3 far1* mutants were much higher than those of *far1-2* and the wild type (Figure 2C). Most strikingly, when the etiolated seedlings were exposed to short periods of high light (1000 μmol m^{-2} s^{-1} for 5 h) followed by normal light (150 μmol m^{-2} s^{-1}), 20 and 50% of *fhy3-4* and *fhy3 far1*, respectively, turned green, whereas only 2% of *far1-2* and <1% of wild-type seedlings survived (Figure 2D). In addition, DEX treatment

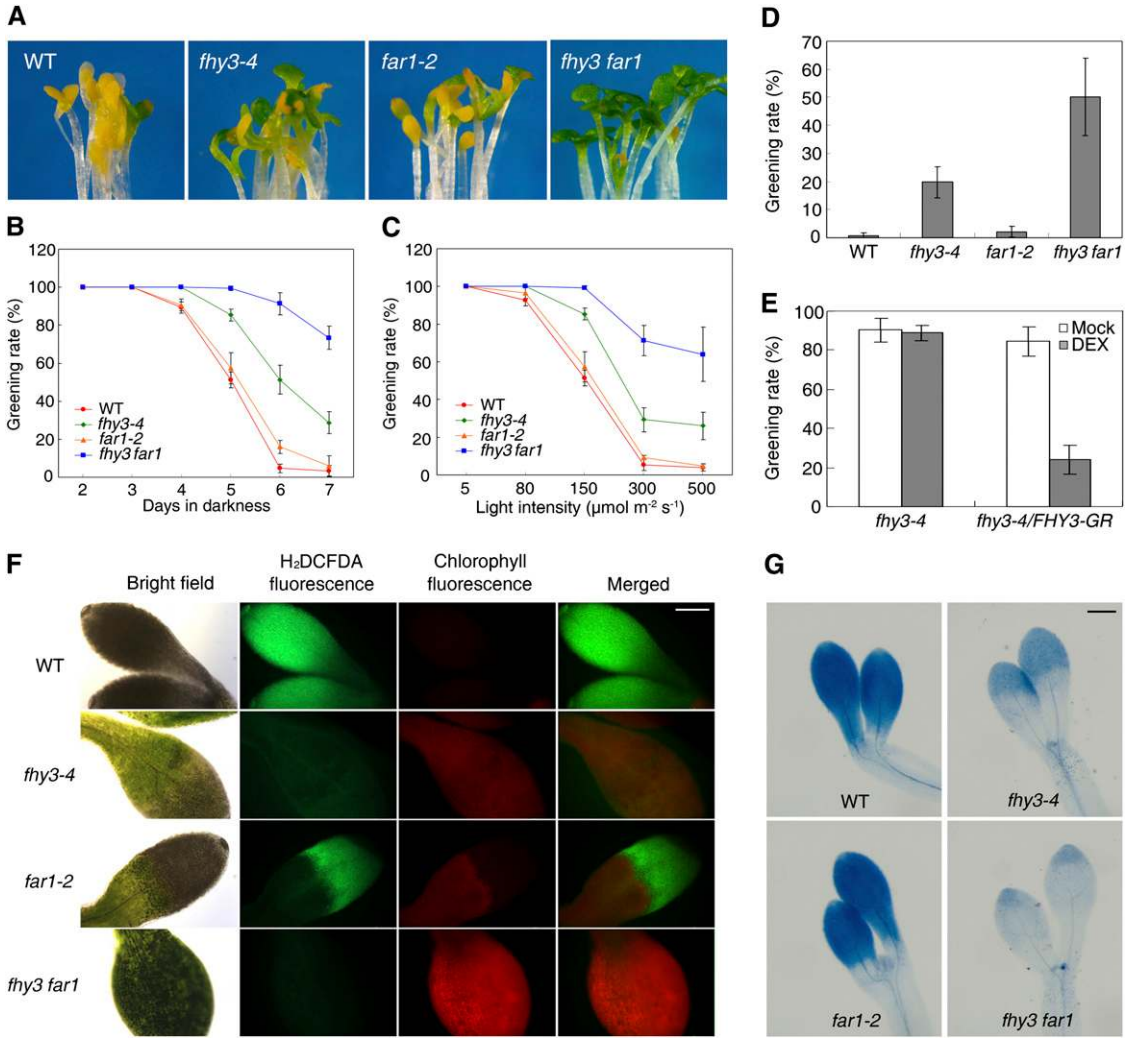

Figure 2. Loss of FHY3/FAR1 Enhances Seedling Greening and Prevents Photobleaching during Deetiolation.

(A) Representative images of 6-d-old etiolated seedlings when exposed to light for 2 d. WT, the wild type.
(B) Percentage of green cotyledons of seedlings grown in various time periods of darkness before being moved to 150 μmol m^{-2} s^{-1} white light for 2 d.
(C) Greening rates of 5-d-old etiolated seedlings transferred to various intensities of white light for 2 d.
(D) Greening rate of 5-d-old etiolated seedlings transferred to high light (1000 μmol m^{-2} s^{-1}) for 5 h followed by 150 μmol m^{-2} s^{-1} for additional 2 d.
(E) Greening rate of 5-d-old *fhy3-4/FHY3-GR* transgenic and *fhy3-4* mutant seedlings grown in darkness in the absence (Mock) or presence of 1 μM DEX followed by 2 d of 150 μmol m^{-2} s^{-1} light exposure. Data in **(B)** to **(E)**, mean ± SD, $n = 3$.
(F) Fluorescence microscope images of ROS (indicated by H_2DCFDA fluorescence) and chlorophyll autofluorescence in the cotyledons of 5-d-old etiolated seedlings followed by 2 d of 150 μmol m^{-2} s^{-1} light treatment.
(G) Trypan blue staining of 6-d-old etiolated seedlings exposed to 150 μmol m^{-2} s^{-1} light for an additional 2 d. Bars in **(F)** and **(G)** = 200 μm.

greatly restored the greening phenotype of *fhy3-4/FHY3p:FHY3-GR* transgenic seedlings (Figure 2E). These data indicate that FHY3 and FAR1 play an important role in seedling greening during deetiolation.

Upon light illumination, excess Pchlide may generate ROS or free radicals, resulting in photobleaching or even cell death in the cotyledons (Reinbothe et al., 1996; Buhr et al., 2008). To test whether the increased greening rate of the mutants is the result of less photobleaching, we investigated ROS production by detecting 2′,7′-dichlorodihydrofluorescein diacetate (H_2DCFDA) fluorescence of the cotyledons (Zhong et al., 2009). We found that H_2DCFDA fluorescence was remarkably lower in the *fhy3-4* and *fhy3 far1* mutants and slightly lower in *far1-2* than that in the wild type. However, chlorophyll autofluorescence was obvious in *fhy3-4* and *fhy3 far1* (Figure 2F). Furthermore, when stained with trypan blue (indicating dead cells), the cotyledons of the wild type and *far1* were stained blue, whereas *fhy3* and *fhy3 far1* seedlings were barely stained (Figure 2G). Therefore, disruption of *FHY3* and *FAR1* prevents photobleaching and cell death.

FHY3 Activates *HEMB1* Expression by Directly Binding to Its Promoter

The observed phenotypes prompted us to test whether the expressions of tetrapyrrole biosynthetic genes were influenced by FHY3 and FAR1 (see Supplemental Figure 3A online). *fhy3 far1* double mutant and wild-type seedlings were grown in darkness for 5 d, and relative gene expression was analyzed by quantitative RT-PCR (qRT-PCR). We found that only a small set of genes, including *HEMA3*, *HEMB1*, *FERROCHELATASE 2* (*FC2*), *HEME OXYGENASE 1* (*HO1*), *HO3*, and *HO4*, were either up- or downregulated more than 1.5-fold in the *fhy3 far1* double mutant compared with the wild type (see Supplemental Figure 3B online). It was previously shown that FHY3 activates downstream gene expression mainly through binding the FHY3/FAR1 binding site (FBS) (CACGCGC) present in promoters of its targets (Lin et al., 2007; Li et al., 2011). Therefore, we surveyed the promoter sequences of these tetrapyrrole biosynthetic genes and found that only *HEMB1* contains a putative FBS motif, which is located 385 bp upstream of the ATG start code in reverse orientation (Figure 3A). To investigate whether FHY3 and FAR1 could bind to the *HEMB1* promoter through this putative FBS motif, we first used a yeast one-hybrid system. GAD-FHY3 (fused with GAL4 activation domain) and GAD-FAR1 proteins were able to bind the wild-type *HEMB1* oligonucleotide containing the FBS sequence (*HEMB1wt*:*LacZ*) and activate *LacZ* reporter gene expression, but they did not bind the mutant oligonucleotide (*HEMB1m*:*LacZ*, in which GCGCGTG was changed into GCttGTG) (Figure 3B). Next, we performed electrophoresis mobility shift assay (EMSA) to test whether FHY3 binds the *HEMB1* promoter fragment in vitro. Our data showed that the FHY3 recombinant protein (N-terminal 250 amino acids of FHY3 fused with glutathione *S*-transferase; GST-FHY3N) caused an upshift band with *HEMB1* wild-type oligonucleotides labeled with ^{32}P, and this band was abolished by excess unlabeled wild-type oligonucleotides but not by excess unlabeled mutant oligonucleotides (Figure 3C). To investigate further whether FHY3 binds *HEMB1* DNA fragment in vivo, chromatin immunoprecipitation (ChIP) was performed using 35S:*GUS-FHY3* (GUS for β-glucuronidase) transgenic seedlings (Wang and Deng, 2002). The ChIP DNA was quantified by real-time PCR with three sets of primers spanning the upstream promoter,

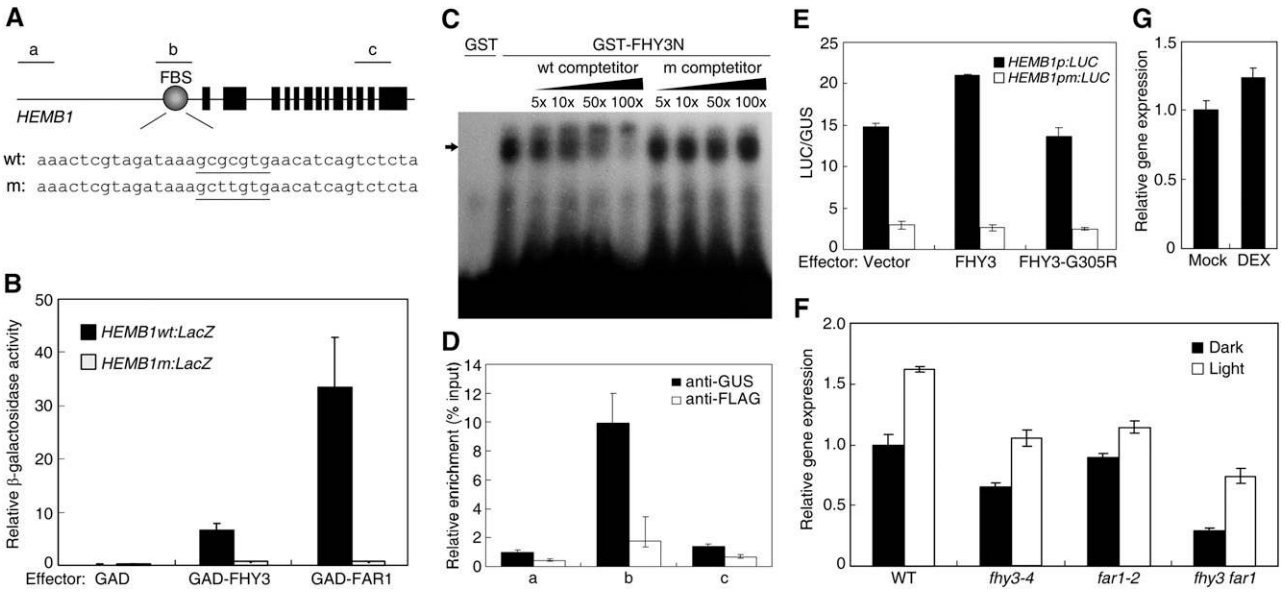

Figure 3. FHY3/FAR1 Bind to the Promoter of *HEMB1* and Activate Its Gene Expression.

(A) A schematic diagram of the *HEMB1* gene. Black rectangles represent exons, and gray circle indicates the FBS motif. Wild-type (wt) and mutant (m) oligonucleotide sequences are shown below, and the FBS motif sequence is underlined. a, b, and c indicate fragments for ChIP-PCR.

(B) Relative β-galactosidase activities of *LacZ* reporters (*HEMB1wt*:*LacZ* and *HEMB1m*:*LacZ*) activated by GAD-fused effectors in the yeast one-hybrid assay. Mean ± SD, $n = 6$.

(C) EMSA assay of GST-FHY3N or GST recombinant proteins incubated with ^{32}P-labled wild-type oligonucleotides in the presence of a series of excess amounts of wild-type or mutant unlabeled competitors. Arrow indicates shifted bands of protein-DNA complexes.

(D) ChIP assay of 5-d-old etiolated *35S*:*GUS-FHY3* transgenic seedlings. Samples were precipitated with anti-GUS antibody (GUS) or anti-FLAG antibody (negative control). ChIP DNA was quantified by real-time PCR with primers targeting fragments as shown in **(A)**. Mean ± SD, $n = 3$.

(E) Transient activation assay of luciferase reporter gene driven by the wild type (*HEMB1p*:*LUC*) or mutant (*HEMB1pm*:*LUC*, in which the FBS motif was mutated) *HEMB1* promoter in protoplasts. Protoplast transformation and incubation were conducted in weak light. Relative activity is expressed as the ratio of LUC versus GUS internal control. Mean ± SD, $n = 3$.

(F) *HEMB1* expression in 5-d-old dark-grown seedlings transferred to light or kept in darkness for 6 h. WT, the wild type.

(G) *HEMB1* expression in *FHY3-GR* transgenic seedlings treated without (Mock) or with 1 μM DEX. Relative expression levels are normalized to that of *UBQ*. Mean ± SD from three biological replicates in **(F)** and **(G)**.

the FBS motif, and the coding region, respectively. Our results showed that only the "b" fragment containing FBS motif was significantly enriched in samples precipitated by anti-GUS antibody but not in samples pulled down by anti-FLAG negative control (Figure 3D). Together, these results confirm that FHY3 directly binds to the *HEMB1* promoter in an FBS motif–dependent manner.

A previous study demonstrated that FHY3 and FAR1 possess intrinsic transcriptional activation activity (Lin et al., 2007). We then examined how FHY3 regulates the downstream gene expression by cotransforming a luciferase (*LUC*) reporter gene driven by the *HEMB1* promoter (1.5 kb upstream of ATG) with various effectors into *Arabidopsis* protoplasts. Our transient expression assay showed that FHY3 protein was able to activate *LUC* reporter gene expression (Figure 3E). However, a point mutation in the transposase domain of FHY3 (FHY3-G305R; deficient in transcriptional activation; Lin et al., 2007) failed to activate *LUC* expression (Figure 3E). When *LUC* was driven by the *HEMB1* promoter with mutations in the FBS motif, the expression level was drastically reduced and FHY3 was no longer able to activate it (Figure 3E). Next, using qRT-PCR analysis, we found that *HEMB1* expression was modestly decreased in *far1-2* and further dropped in *fhy3-4*, whereas it was significantly decreased in *fhy3 far1* (Figure 3F), suggesting that FHY3 and FAR1 redundantly upregulate *HEMB1* expression. In addition, DEX treatment also promoted *HEMB1* expression in the *FHY3p*:*FHY3-GR* transgenic plants compared with the mock treatment (Figure 3G). We thus conclude that FHY3 and FAR1 positively regulate *HEMB1* gene expression in plant cells.

FHY3/FAR1 Promote ALAD Activity

HEMB1 is one of two genes encoding ALAD, which catalyzes a reaction among the early steps of tetrapyrrole biosynthesis. We then examined how the ALAD protein level and enzymatic function were affected by *fhy3* and *far1* mutations. To this end, a polyclonal antibody against a peptide (amino acids 336 to 346) of ALAD was raised in rabbit. This antibody recognized the ALAD recombinant protein at a size of 55 kD, which is close to the predicted size of the ALAD mature protein, confirming the specificity of this antibody (see Supplemental Figure 4A online). Compared with wild-type plants, the ALAD protein level in *far1-2* was slightly reduced, whereas it was clearly decreased in *fhy3-4* and further reduced in *fhy3 far1* double mutant seedlings (see Supplemental Figure 4B online), correlating well with the reduced *HEMB1* transcripts in these mutants (Figure 3F).

To determine how ALAD function was affected, an in vitro enzymatic activity assay was performed in a reaction system containing both the plant protein extracts and ALA substrate, and PBG production was determined (Vajpayee et al., 2000). We found that less PBG was formed with proteins extracted from *far1-2*, and much less was formed from those of *fhy3-4* and *fhy3 far1* compared with the wild type (Figure 4A). Next, 5-d-old etiolated seedlings were fed exogenous 10 mM ALA for 12 h and the ALAD conversion ability was tested in vivo. As shown in Figure 4B, significantly less PBG was detected in the *fhy3-4* and *fhy3 far1* mutants than in the wild-type seedlings. To assess the physiological response further, we grew the plants with or without ALA feeding for 3 d and measured the Pchlide content as well as greening ability after light exposure. Without exogenous ALA treatment, Pchlide levels and greening rates were indistinguishable between *fhy3 far1* and the wild type. However, when fed with ALA, wild-type seedlings contained drastically increased Pchlide, whereas *fhy3 far1* accumulated only half that of the wild type (Figure 4C). Accordingly, almost all of the wild-type cotyledons were severely photobleached, whereas ~75% of the *fhy3 far1* mutant seedlings were still able to turn green after light exposure (Figure 4D). These results firmly demonstrate that the ability to convert ALA into PBG in *fhy3* and particularly *fhy3 far1* mutants was reduced; therefore, FHY3 and FAR1 positively regulate ALAD function in plants.

Constitutive Expression of *HEMB1* Rescues the *fhy3 far1* Mutant Phenotypes

We then determined whether restoration of *HEMB1* in the *fhy3 far1* mutant could rescue its phenotype by constitutively expressing the *HEMB1* ORF under the control of the cauliflower mosaic virus 35S promoter (*35S*:*HEMB1*). Multiple T1 resistant transgenic lines were obtained. Unexpectedly, all T2 transgenic lines segregated with nearly one-fourth of plants developing partially white leaves when grown in soil after 3 weeks (two lines were shown; Figure 5A). The *HEMB1* transcripts in the transgenic lines were more than eightfold higher than those in the mutant (Figure 5B). These plants were eventually died and we were unable to obtain homozygous plants. Strikingly, we observed that the heterozygotes of *HEMB1* overexpression plants rescued the Pchlide accumulation and seedling greening phenotypes of the *fhy3 far1* mutant (Figures 5C and 5D), further confirming that the function of FHY3 and FAR1 in Pchlide synthesis and seedling greening is through the regulation of *HEMB1*. Consistent with this, *HEMB1* is highly expressed in cotyledons during dark-to-light transition (see Supplemental Figure 5 online).

Overexpression, Absence, or Reduction of *HEMB1* Impairs Plant Growth and Development

Similar to what was observed in the *fhy3 far1* mutant background, the homozygous transgenic plants of *35S*:*HEMB1* overexpression lines in the wild type displayed photobleached leaves and did not survive (see Supplemental Figure 6 online). We speculated that *HEMB1* might play essential role in regulating plant growth and development. To test this hypothesis, we obtained a T-DNA insertion mutant allele, Salk_016544, from the ABRC. This allele contains a T-DNA inserted into the eighth intron of *HEMB1*, and the insertion site was sequence confirmed, thereafter it was designated *hemb1-1* (see Supplemental Figures 7A and 7B online). When the heterozygous progeny of *hemb1-1* were grown on Murashige and Skoog (MS) plates containing 50 mg/mL kanamycin, nearly two-thirds (494 out of 747, P value > 0.75 by *t* test) of the seeds were resistant and developed normal seedlings. We attempted to use PCR genotyping to identify homozygotes from those kanamycin-resistant plants. However, all of the resistant plants were heterozygous, suggesting that the *hemb1-1* mutation might be lethal in the

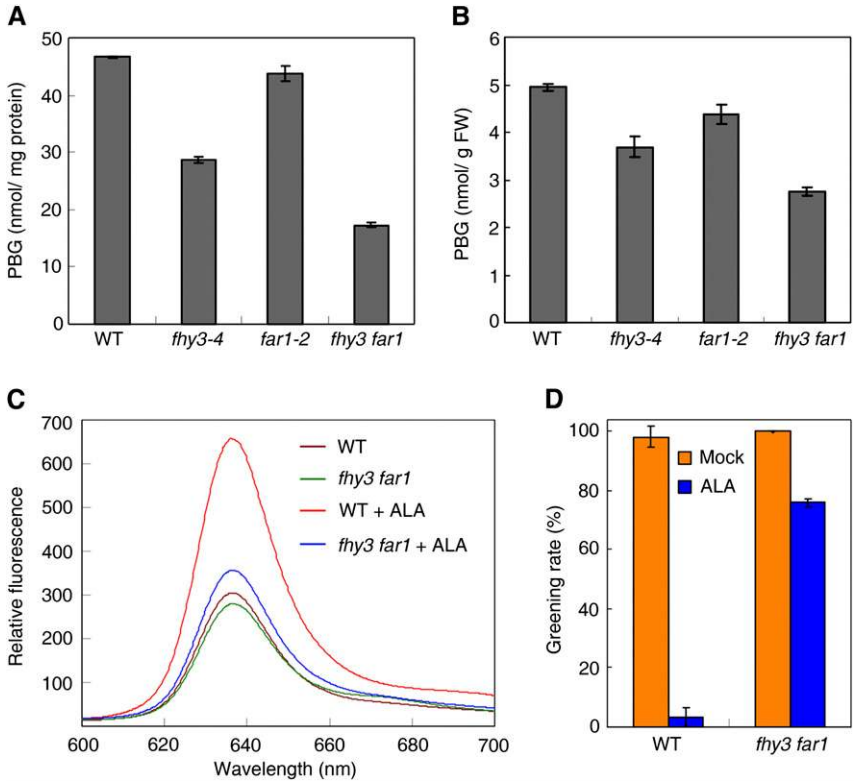

Figure 4. FHY3/FAR1 Promote ALAD Activity.

(A) In vitro ALAD enzymatic assay. Total proteins were extracted from 4-d-old etiolated seedlings and incubated with 100 μM ALA for 2.5 h. WT, the wild type.
(B) In vivo PBG formation of 4-d-old etiolated seedlings fed with 10 mM ALA for 12 h. FW, fresh weight.
(C) and **(D)** Relative Pchlide fluorescence **(C)** and greening rate **(D)** of 3-d-old etiolated seedlings fed with or without 100 μM ALA. Seedlings were exposed to white light for 2 d in **(D)**.
For **(A)**, **(B)**, and **(D)**, mean ± SD, $n = 3$.

homozygous state. Then we dissected the developing siliques and scored the seeds under a dissecting microscope. In wild-type siliques, seeds were fully developed, whereas in 37 siliques from individual *hemb1-1* heterozygous plants grown under the same conditions as the wild-type plants, 359 out of 1351 ovules were small, shrunken, and aborted (Figure 6A). The ratio of nonaborted seeds to aborted seeds was ~3:1 (P value > 0.1). The lethality of the homozygous mutation was complemented by expressing *HEMB1p:HEMB1* (Figure 6A). Taken together, we conclude that *hemb1-1* is a recessive embryo lethal mutation. To dissect precisely the stage of embryogenesis during which the *hemb1* mutant arrests development, embryos within individual immature siliques from self-pollinated *hemb1-1* plants were cleared and examined under a microscope. The normal embryos underwent typical developmental stages, ranging from preglobular, globular, heart, torpedo, and mature. However, the mutant embryos were arrested at the globular stage (see Supplemental Figure 7C online).

We then attempted to use RNA interference (RNAi) and artificial microRNA (amiRNA) transgenic approaches to knock down the endogenous *HEMB1* expression in the Nossen wild-type background. When T1 seeds were germinated on 50 mg/L hygromycin plates, surprisingly, all of the *HEMB1-RNAi* (159 lines) and *HEMB1-amiRNA* (112 lines) resistant seedlings developed white or pale cotyledons. These seedlings did not develop true leave even when grown in MS medium supplied with 2% Suc (Figure 6B). We collected these resistant seedlings and tested the *HEMB1* expression by qRT-PCR, finding that the endogenous *HEMB1* transcripts in those *HEMB1-RNAi* or *HEMB1-amiRNA* lines were severely reduced to <20% of those in the wild type (Figure 6C). These results revealed that severe reduction of *HEMB1* mRNA causes seedling lethality. Taken together, our genetic data confirm that *HEMB1* is critical for plant development and its transcript level has to be precisely maintained.

FHY3 Physically Interacts with PIF1

It has been shown that etiolated *pif1* mutant seedlings overaccumulate Pchlide and are sensitive to photobleaching (Huq et al., 2004; Moon et al., 2008). Here, we found that the *fhy3* and *fhy3 far1* mutants display opposite phenotypes to those of *pif1*. To investigate how the two types of proteins, FHY3/FAR1 and PIF1, antagonistically regulate chlorophyll biosynthesis, we

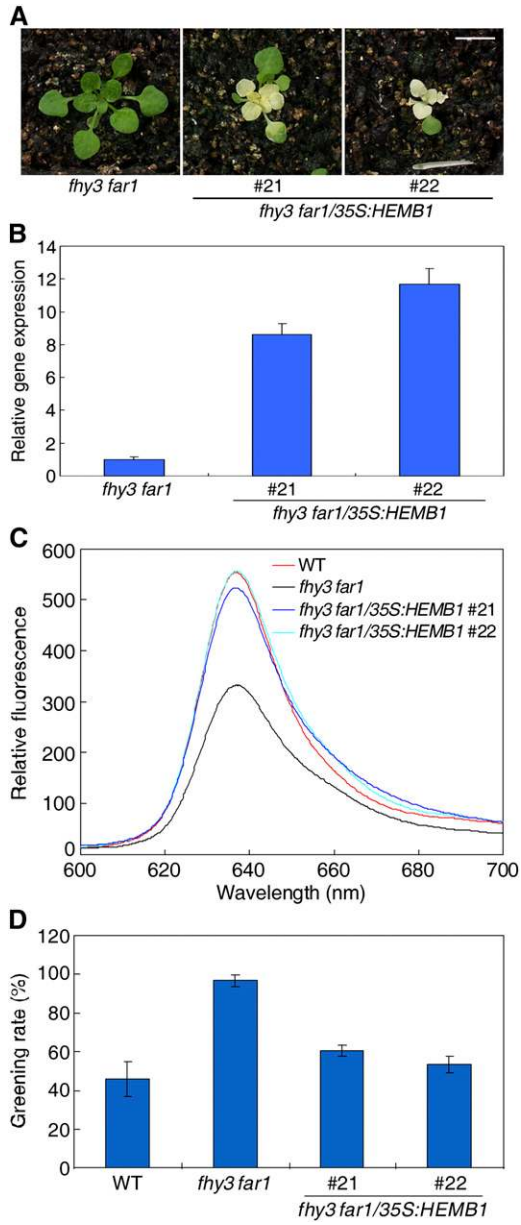

Figure 5. Constitutive Expression of *HEMB1* Rescues the *fhy3 far1* Mutant Phenotypes.

(A) Images of *fhy3 far1/35S:HEMB1* homozygous transgenic plants (two lines are presented) showing white and bleached leaves when grown in soil for 3 weeks (16 h light/8 h dark). Bar = 1 cm.

(B) qRT-PCR showing high expression of *HEMB1* in the transgenic lines. The expression levels were normalized to a *UBQ* endogenous control. Mean ± SD from three biological replicates.

(C) Relative Pchlide levels of 5-d-old etiolated seedlings. WT, the wild type.

(D) Greening rate of 5-d-old etiolated seedlings following 2 d of light exposure. Mean ± SD, $n = 3$.

constructed *fhy3 pif1* double and *fhy3 far1 pif1* triple mutants by genetic crossing. We found that the low Pchlide levels in the *fhy3* and *fhy3 far1* mutant seedlings were partially repressed by the *pif1* mutation in darkness (Figures 1A and 7A). When 4-d-old etiolated seedlings were exposed to light for 2 d, the greening rates of *fhy3 pif1* and *fhy3 far1 pif1* mutants were ~26 and 70%, respectively, whereas the *pif1* mutant cotyledons were severely photobleached (Figure 7B). These results indicate that PIF1 partly suppresses the function of FHY3/FAR1 in regulating Pchlide accumulation and seedling greening.

It was then intriguing to ask whether there could be direct interaction between FHY3 and PIF1. The N-terminal domain of FHY3 has been shown to interact with HY5, CIRCADIAN CLOCK-ASSOCIATED1 (CCA1), and LATE ELONGATED HYPOCOTYL (LHY) proteins previously (Li et al., 2010; Li et al., 2011). We first performed a yeast two-hybrid assay using bait vector expressing the N-terminal 250 amino acids of FHY3 with the LexA DNA binding domain (LexA-FHY3N) and prey vector

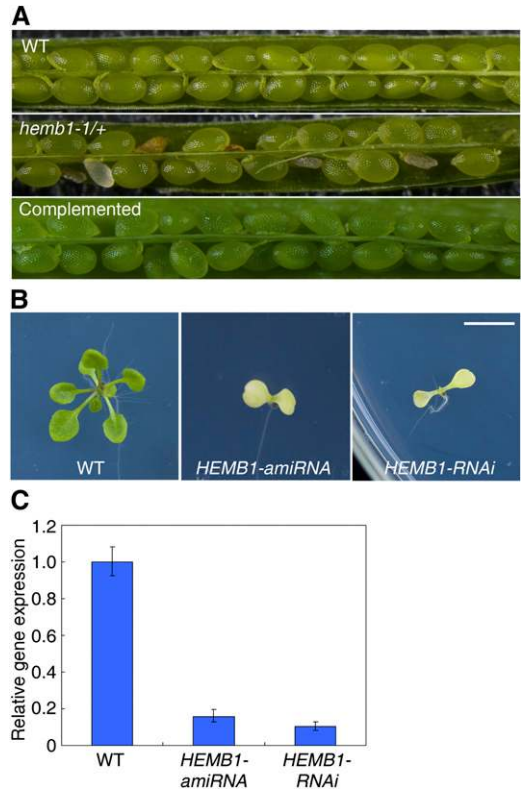

Figure 6. Absence or Reduction of *HEMB1* Impairs Plant Growth and Development.

(A) A heterozygous *hemb1-1* mutant silique showing that approximately one-quarter of the embryos are aborted compared with the wild type (WT) and complemented transgenic siliques.

(B) Pale cotyledons of *HEMB1-amiRNA* and *HEMB1-RNAi* transgenic seedlings grown on MS plates for 2 weeks. One representative line for each construct is shown. Bar = 0.5 cm.

(C) qRT-PCR showing extremely low expression of *HEMB1* in the transgenic lines as in **(B)**. The expression levels are normalized to an *UBQ* endogenous control. Mean ± SD from three biological replicates.

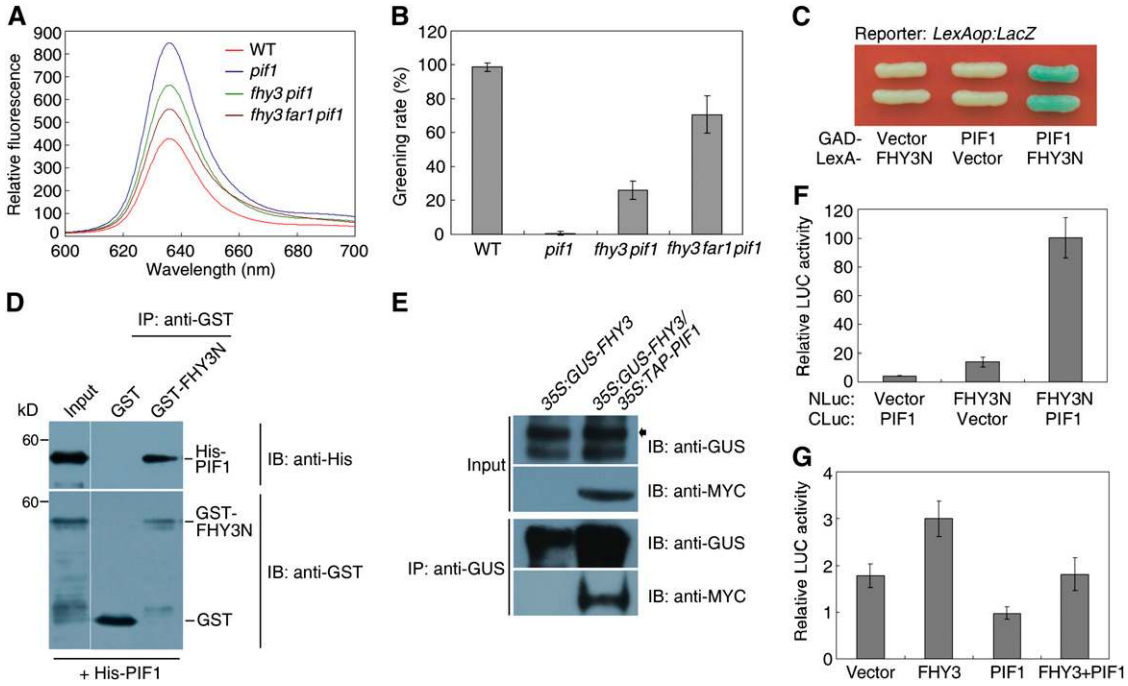

Figure 7. FHY3 Directly Interacts with PIF1.

(A) Relative fluorescence indicating Pchlide accumulation in 4-d-old etiolated seedlings. WT, the wild type.
(B) Percentage of seedlings with green cotyledons when 4-d-old etiolated seedlings were exposed to white light for 2 d. Mean ± SD, $n = 3$.
(C) A yeast two-hybrid assay for interaction between GAD-fused PIF1 and LexA-fused N-terminal fragment of FHY3 (1 to 250 amino acids, FHY3N).
(D) In vitro pull-down assay between His-tagged PIF1 and GST-fused FHY3N. The His-PIF1 proteins were incubated with immobilized GST or GST-FHY3N, and immunoprecipitated fractions were probed with an anti-His or anti-GST antibody. IB, immunoblot; IP, immunoprecipitation.
(E) Coimmunoprecipitation assay between GUS-FHY3 and TAP-PIF1 in vivo. Seedlings were grown in darkness for 4 d. After precipitation with anti-GUS antibody, proteins were immunoblotted with anti-GUS or anti-MYC antibodies. Arrow indicates GUS-FHY3 bands.
(F) LCI assay between FHY3N and PIF1 fused with the N-terminal or C-terminal fragment of firefly luciferase, respectively. Relative LUC activity is normalized to *35S*:*GUS* internal control. Mean ± SD, $n = 3$.
(G) Relative *HEMB1p*:*LUC* reporter activity in *Arabidopsis* protoplasts cotransformed with the effector constructs. The relative LUC activities were normalized to the *35S*:*GUS* internal control. Mean ± SD, $n = 3$. Protoplast transformation, incubation, and protein extraction were performed in darkness (**[F]** and **[G]**).

expressing full-length PIF1 with the GAL4 activation domain (GAD-PIF1). Our data showed that LexA-FHY3N indeed interacts with GAD-PIF1, and the N-terminal domain containing the C2H2 zinc finger motif is responsible for mediating the interaction (Figure 7C). We further performed a pull-down analysis between recombinant 6×His-fused PIF1 (His-PIF1) and GST-tagged FHY3N (GST-FHY3N) and found that GST-FHY3N, but not GST alone, was able to pull down PIF1 in vitro (Figure 7D). Next, we examined the in vivo interaction between FHY3 and PIF1. Transgenic plants expressing *35S*:*GUS-FHY3* together with *35S*:*TAP-PIF1* were used for coimmunoprecipitation assays. As shown in Figure 7E, GUS-FHY3 was able to precipitate TAP-PIF1 in planta. Furthermore, firefly LUC complementation imaging (LCI) assays (Chen et al., 2008) were conducted by transiently expressing FHY3N-NLuc (or FHY3-NLuc) and CLuc-PIF1 fusions in *Arabidopsis* protoplasts. We found that coexpression of FHY3N-NLuc and CLuc-PIF1 reconstituted strong LUC activity, but the controls did not (Figure 7F). In addition, cotransformation of FHY3-NLuc with CLuc-PIF1 also led to LUC activity (see Supplemental Figure 8A online). Taken together, these data indicate that FHY3 physically interacts with PIF1 through its N-terminal domain.

As shown earlier, FHY3 activates *HEMB1* expression in plant cells; we then ask whether FHY3-PIF1 interaction could influence *HEMB1* expression. To this end, we cotransformed FHY3 (*35S*:*FHY3*) and/or PIF1 (*35S*:*PIF1*) effectors together with *HEMB1p*:*LUC* reporter construct in *Arabidopsis* protoplasts. Our data showed that PIF1 alone inhibited the transcription of the *LUC* reporter gene. Coexpression of PIF1 largely suppressed the activation activity of FHY3 on the *HEMB1p*:*LUC* reporter (Figure 7G). Consistent with this, the *HEMB1* transcript level in *fhy3 far1* mutant was largely derepressed by the *pif1* mutation (see Supplemental Figure 8B online). These results demonstrate that PIF1 interferes with FHY3/FAR1-activated *HEMB1* transcription.

FHY3 Is Upregulated by White Light

To assess how expressions of *FHY3* and *FAR1* themselves are regulated during deetiolation, 4-d-old etiolated wild-type seedlings were transferred to white light in a time course. Real-time

RT-PCR analysis showed that the *FHY3* transcript level was elevated after light treatment for 6 h, whereas *FAR1* gene expression was slightly affected by light (Figure 8A). To investigate the regulation of FHY3 protein, dark-grown *35S*:*GUS-FHY3* transgenic seedlings were exposed to light and GUS activity was determined. We found that the GUS activity was increased along with light treatment (Figure 8B). Moreover, by bioluminescence analysis of the *FHY3p*:*FHY3-LUC* reporter gene, we further showed that the FHY3 level was increased in white light (see Supplemental Figure 9A online). Consistent with being the direct target of FHY3/FAR1, the *HEMB1* transcript was induced by light partly dependent on FHY3/FAR1. Its protein content was also increased in wild-type plants upon light illumination (see Supplemental Figures 9B and 9C online). These findings indeed support the positive role of FHY3 in regulating chlorophyll biosynthesis.

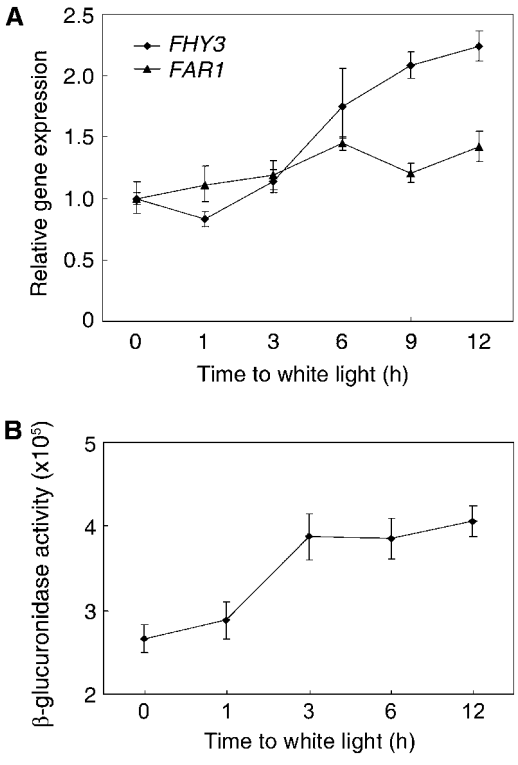

Figure 8. FHY3 Is Upregulated by White Light.

(A) *FHY3* and *FAR1* gene expression by real-time RT-PCR analysis. Four-day-old etiolated wild-type seedlings were transferred to white light for various time periods. Relative expression levels are normalized to those of *UBQ*. Mean ± SD from three biological replicates.

(B) GUS activity assay showing relative FHY3 protein level in 4-d-old etiolated *35S*:*GUS-FHY3* transgenic seedlings after light illumination. Mean ± SD of 50 seedlings, $n = 3$.

DISCUSSION

FHY3/FAR1 Are Key Components That Positively Regulate Chlorophyll Biosynthesis

The tetrapyrrole biosynthetic pathway is finely regulated at multiple levels, and some negative regulators have been reported in plants (Tanaka and Tanaka, 2007). In this study, we provide an array of evidence to show that two transposase-derived transcription factors, FHY3 and FAR1, positively regulate chlorophyll biosynthesis through directly activating *HEMB1* gene expression. First, yeast one-hybrid, EMSA and ChIP experiments demonstrate that FHY3 protein directly binds to the promoter of *HEMB1* and that the typical FBS *cis*-element in the promoter is responsible for mediating the binding. Second, FHY3 activates *HEMB1* transcription in an FBS motif–dependent manner in protoplast transient expression assays. Third, *HEMB1* gene expression and in vitro and in vivo ALAD catalytic activities are reduced by *fhy3* and *far1* mutations (Figures 3 and 4). Consistent with these molecular data, *fhy3*, *far1*, and *fhy3 far1* mutants accumulate less Pchlide than the wild type in darkness (Figure 2). In the tetrapyrrole biosynthetic pathway, *HEMB1* is a unique gene that not only has a typical FBS motif in its promoter but also belongs to a small set of genes that are regulated by FHY3 and FAR1. Our study indeed suggests that *HEMB1* defines a key direct target of FHY3 and FAR1 for transcriptional activation. It should be noted that *HEMC* and *CHLG* were reported as putative FHY3 targets by a ChIP sequence approach (Ouyang et al., 2011). We find that FHY3 and FAR1 have minor effects on the expression of *HEMC* and *CHLG* (see Supplemental Figure 3 online). The discrepancy could be due to the different transgenic plants (*35S*:*3FLAG-FHY3-3HA* in Ouyang et al. [2011] and *35S*:*GUS-FHY3* in this study) and growth conditions used in the two studies.

Seedling survival during the transition from skotomorphogenesis to photomorphogenesis is important for land plants particularly under light stress environments. Targeting genes in the early steps of the biosynthetic pathway for regulation might provide seedlings potential advantages because excess accumulation of photosensitizers (such as Pchlide) of the later steps may generate ROS upon initial light exposure (Tanaka and Tanaka, 2007; Solymosi and Schoefs, 2010). The size of the Pchlide pool must be stoichiometrically linked to the amount of POR enzymes (Runge et al., 1996; Buhr et al., 2008). Thus, Pchlide content in darkness has to be maintained at relatively low level in preparation for rapid transition. ALA formation is the rate-limiting step of the entire pathway, and GluTR activity is tightly regulated (Mochizuki et al., 2010). For example, failure to repress GluTR activity in the dark results increased accumulation of Pchlide in the *flu* mutant (Goslings et al., 2004). *HEMB1* functions just after ALA formation among the common steps in the tetrapyrrole biosynthetic pathway. Our data quantitatively and collectively demonstrate that different degrees of Pchlide accumulation (Figure 1A) and photobleaching (Figure 2) phenotypes correlate with the transcript level of *HEMB1* (Figure 3F), ALAD protein level (see Supplemental Figure 4B online), and enzyme activity (Figures 4A and 4B) in the *far1*, *fhy3*, and *fhy3 far1* mutants. On the other hand, the endogenous *HEMB1* level might be subject to fine regulation (see below in detail). We thus

believe that a low-fold gene expression change of *HEMB1* is likely sufficient to trigger the drastic seedling greening phenotype in the *fhy3 far1* mutant. In *Arabidopsis*, ALAD is encoded by *HEMB1* and *HEMB2*. *HEMB1* is greatly induced in cotyledons during dark-to-light transition and expressed in all tissues and developmental stages examined. However, the expression of *HEMB2* is barely detected (see Supplemental Figure 5 online), suggesting that *HEMB1* is the major contributor at this step. This notion is further supported by genetic study showing that constitutive expression of *HEMB1* rescues the *fhy3 far1* mutant phenotypes (Figure 5). A previous study showed that FHY3 and FAR1 regulate chloroplast development through activating *ARC5* expression (Ouyang et al., 2011). However, an *arc5* loss-of-function mutant did not show differences in Pchlide level or greening ability relative to Landsberg *erecta* wild type (see Supplemental Figure 10 online), indicating that ARC5 is not involved in the regulation of chlorophyll biosynthesis during deetiolation.

Most strikingly, FHY3 expression is repressed in darkness, and light induces its expression probably through activating phytochrome signaling. Therefore, we propose a model in which, in darkness, less *HEMB1* is induced by FHY3 (and FAR1), resulting in small pool of Pchlide. After light irradiation, increased FHY3 levels activate *HEMB1* expression, thereby promoting the conversion of ALA to PBG and subsequent Pchlide accumulation for chlorophyll synthesis and photoautotrophic growth (Figure 9).

When excess Pchlide accumulates in the dark-grown seedlings, POR represents a critical regulatory layer for the control of chlorophyll biosynthesis during seedling greening. In agreement with this, *ga1-3* and *gai* mutant seedlings showed increased *POR* expression and were more resistant to photooxidative damage, despite a high accumulation of Pchlide in the dark (Cheminant et al., 2011). Moreover, overexpression of *POR* promoted seedling greening (Sperling et al., 1997; Cheminant et al., 2011). By contrast, reduction of *POR* expression in the *pif1* and *ein3* mutants resulted in severe photobleaching during dark-to-light transition (Moon et al., 2008; Zhong et al., 2009).

Interestingly, we observed that mutations in *fhy3* and *far1* do not alter the nonbound heme content, probably through opposite regulation of *FC2*, *HO1*, *HO3*, and *HO4* genes that act in the heme branch. Thus, it is postulated that FHY3 and FAR1 specifically contribute to the chlorophyll biosynthetic pathway. This is in agreement with the idea that newly synthesized tetrapyrroles need to be directed to the chlorophyll branch rather than the heme branch during initial seedling greening (Stephenson and Terry, 2008).

Integration of Two Distinct Types of Transcription Factors in Chlorophyll Biosynthesis Regulation

The discovery of positive regulators is of utmost significance for understanding the exquisite regulation of the chlorophyll biosynthetic pathway. In this study, we find that by means of its N-terminal domain FHY3 physically interacts with PIF1, a phytochrome-interacting transcription factor (Figure 7). The *pif1* mutant accumulates extremely high levels of Pchlide in the dark, and PIF1 has been revealed as a negative regulator of chlorophyll biosynthesis (Huq et al., 2004; Moon et al., 2008). Although

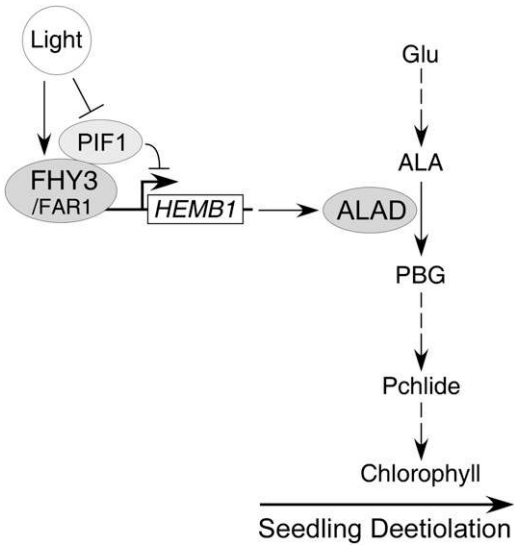

Figure 9. A Model for the Role of FHY3/FAR1 in Regulating Chlorophyll Biosynthesis.

FHY3 and FAR1 bind to the promoter and activate the expression of *HEMB1* (encoding the ALAD enzyme), with FHY3 playing a predominant role. In darkness, FHY3 is maintained at a relatively low level, so that less Pchlide accumulates in cotyledons. Light promotes FHY3 expression, thereby increasing *HEMB1* transcript and ALAD protein levels, allowing Pchlide accumulation and subsequent chlorophyll formation. Meanwhile, PIF1 interferes with the activation activity of FHY3 (and FAR1) by physically interacting with FHY3. Light releases this repression by proteasome-mediated degradation of PIF1. Arrows, positive regulation; bars, negative regulation. Arrows with dash lines indicate multiple steps.

PIF1 may indirectly regulate *GUN5* expression (Shin et al., 2009), the mechanism of PIF1 in regulating Pchlide synthesis is not well understood. We show that PIF1 directly interacts with FHY3 (and maybe FAR1 as well) and partly represses FHY3 activation activity on *HEMB1* gene expression. It is speculated that the regulation of PIF1 in Pchlide synthesis in the dark may be partly dependent on the function of FHY3/FAR1. Accordingly, the *fhy3 far1* double mutant is largely able to suppress the *pif1* mutant phenotypes (Figure 7). Thus, two distinct types of transcription factors in the phytochrome signaling pathway coordinate to regulate an important biological response. In agreement with this finding, a recent analysis reported that FHY3 and PIF1 (PIL5) coregulate more than 100 genes (Ouyang et al., 2011). They could also be involved in mediating other diverse processes through their interaction. Our finding supports the hypothesis that the expression of genes involved in chlorophyll biosynthesis is regulated by a tight and complex mechanism comprising multiple components (Tanaka and Tanaka, 2007). It also implies that both positive and negative players work coordinately to optimize chlorophyll biosynthesis, thus enabling etiolated seedlings to prepare properly for emerging at the soil surface (Figure 9).

We also noticed that HY5 likely has a positive role in regulating Pchlide synthesis (see Supplemental Figure 1 online). HY5 acts as a key player in light signaling and interacts with FHY3 and FAR1 (Oyama et al., 1997; Li et al., 2010). It will be

interesting to investigate whether FHY3, PIF1, and HY5 work together to coregulate chlorophyll biosynthesis in plants. Recent studies also demonstrated the involvement of FHY3/FAR1 in mediating phyA signaling homeostasis and the circadian clock by cooperating with negative transcription factors, such as HY5, CCA1, and LHY (Li et al., 2010; Li et al., 2011). Hence, integration with a specific transcription repressor(s) in regulating a distinct biological process likely defines a common molecular mechanism underlying FHY3/FAR1 action.

HEMB1 Is Critical for Plant Development

Although *HEMB1* has been cloned from some species (Kaczor et al., 1994; Polking et al., 1995), its function in plant development has not been demonstrated. Our study collected genetic evidence suggesting that besides being a key gene for chlorophyll biosynthesis, *HEMB1* is critical for plant embryonic and postembryonic development. The T-DNA insertion mutation in *HEMB1* is embryo lethal, and the *HEMB1* RNAi and amiRNA transgenic plants display seedling lethality after germination (Figure 6). Other studies have implied that a large number of plastid-targeted proteins are required for proper embryogenesis in *Arabidopsis* (Hsu et al., 2010; Bryant et al., 2011). However, no direct evidence has shown that genes in chlorophyll biosynthesis are involved in regulating embryo development. We speculate that the arrested embryo development of the *hemb1* mutant might be caused by disruption of embryo pigmentation and/or the absence of an essential intermediate(s) of the tetrapyrrole biosynthetic pathway. Moreover, homozygotes of *HEMB1* overexpression lines in either wild-type or *fhy3 far1* mutant backgrounds develop white leaves and are photobleached when grown in soil (Figure 5; see Supplemental Figure 6 online). These data firmly indicate that *HEMB1* is crucial for plant development and its regulation is mainly at the transcriptional level. Consistent with this notion, both Pchlide levels and seedling greening rates correlate well with the *HEMB1* transcript levels in the *far1*, *fhy3*, and *fhy3 far1* mutants (Figures 2 and 3F). When the endogenous *HEMB1* mRNA drops to <20% of the wild type, the RNAi or amiRNA transgenic plants develop only white cotyledons and are not able to survive (Figure 6). Therefore, it is likely that a certain threshold level of *HEMB1* transcript is required for embryos and young seedlings to ensure their viability. In agreement, *HEMB1* is expressed at a relatively high level in the aboveground tissues examined (see Supplemental Figure 5 online).

ALAD is an ancient and conserved protein not only in plants and fungi but also in animals and humans. The deficiency of ALAD in humans results in increased excretion of ALA in the urine, leading to ALAD-deficient porphyria, an autosomal recessive disorder (Maruno et al., 2001). Thus, ALAD activity in neonatal blood is used as a screening tool for ADP (Schulze et al., 2001). The human ALAD gene has two promoter regions that generate different transcripts by alternative splicing, although the enzyme produced is identical, suggesting that it is regulated transcriptionally and posttranscriptionally (Schubert et al., 2009). It is assumed that the functionality and regulatory mechanism of ALAD might be conserved in organisms.

Genetic studies have revealed that some other proteins involved in tetrapyrrole biosynthesis are also essential for plant growth and development. For example, plants with antisense inhibition of *HEMA1* lack chlorophyll and fail to survive under normal growth conditions (Kumar and Söll, 2000). *Arabidopsis* and tobacco (*Nicotiana tabacum*) transgenic etiolated plants with overexpression of *HEMA1* accumulate excessive Pchilde and do not survive after subsequent illumination (Schmied et al., 2011). Absence of GluTRBP is lethal, and mutants with reduced GluTRBP content are photobleached under high light stress (Czarnecki et al., 2011). Similar to *HEMB1*, overexpression of *GUN5*, a gene encoding the ChlH subunit of Mg^{2+}-chelatase, causes spontaneous photobleaching and cell death (Shin et al., 2009). However, unlike *hemb1*, the *gun5* loss-of-function mutant has a pale phenotype and is able to grow in soil (Mochizuki et al., 2001). Therefore, the functionalities of these genes may be overlapping as well as distinct, although they are all required for tetrapyrrole biosynthesis in plants.

METHODS

Plant Materials and Growth Conditions

The *fhy3-4*, *far1-2*, and *fhy3 far1* mutants are of *Arabidopsis thaliana* Nossen ecotype (Hudson et al., 1999; Wang and Deng, 2002; Lin et al., 2007). The *hemb1-1* (Salk_016544), *pif1-2* (Huq et al., 2004), *hy5* (Oyama et al., 1997), *hyh* (cs849765; Kleine et al., 2007), *hfr1* (Yang et al., 2005), *pif3* (Salk_030753; Kim et al., 2003) and *laf1* (Salk_009403C) mutant are in the Columbia (Col) ecotype. The *arc5* mutant is of the Landsberg *erecta* ecotype (Ouyang et al., 2011). *35S*:*GUS-FHY3* (Wang and Deng, 2002), *FHY3p*:*FHY3-GR*, *FHY3p*:*FHY3* (Lin et al., 2007), and *FHY3p*:*FHY3-LUC* (Li et al., 2011) are transgenic lines in the *fhy3-4* mutant background. Double and triple mutants/ transgenic plants were generated by genetic crossing. Homozygous lines were confirmed by genotyping or sequencing. After sterilization, seeds were sown onto MS medium containing 1% Suc and 0.8% agar and were incubated at 4°C in darkness for 3 d, followed by irradiation for 9 h with white light to promote uniform germination.

Greening Rate Measurement

Dark-grown seedlings were transferred to continuous white light (supplied with light-emitting diodes) for 2 d at 22°C or otherwise as indicated in the text. Greening rate was determined by counting the percentage of dark-green cotyledons from 50 to 80 seedlings of each genotype. At least three independent biological repeats were performed.

Pchlide Determination and Fluorescence Imaging of ROS

For Pchlide measurement, 50 seedlings were grown in darkness for 4 or 5 d. The samples were homogenized in 500 μL of ice-cold 80% acetone and incubated in darkness for 4 h. After centrifugation at 5000*g* for 5 min, 150 μL of the supernatant was mixed with 350 μL of glycol. Room temperature fluorescence was excited at 440 nm and scanned from 600 to 700 nm by a fluorescence spectrophotometer (Hitachi). For fluorescence imaging of ROS, seedlings were incubated with 10 μM H_2DCFDA in 10 mM Tris-HCl, pH 7.2, for 10 min as described (Joo et al., 2005). H_2DCFDA and chlorophyll fluorescence images were captured by DMI4500 fluorescence microscope equipped with a charge-coupled device camera (Leica).

Trypan Blue Staining

Seedlings were boiled for 5 min in staining solution (1.8 mL phenol, 2 mL lactic acid, 2 mL glycerol, and 2 mL of 1 mg/mL trypan blue stock solution) and stained overnight. Tissues were mounted on slides and photographed on a dissecting microscope.

Phenotypic Analysis of Embryo Development

Embryos were excised from siliques at different developmental stages and cleared with Herr's solution (Herr, 1971) overnight at 37°C. Samples were mounted between a microscope slide and a cover slip with a drop of Hoyer's solution (7.5 mL water, 1.3 g glycerol, 1.9 g gum arabic crystals and 25 g chloral hydrate) and observed with a microscope (Olympus).

Plasmid Construction

To generate *LacZ* reporter genes driven by the *HEMB1* promoter with a wild-type or mutant FBS motif, the 39-bp oligonucleotides were synthesized as two complementary primers (HEMB1WF and HEMB1WR for the wild type, and HEMB1MF and HEMB1MR for mutant) with an *Eco*RI site overhang at the 5′ end and an *Xho*I site overhang at the 3′ end, respectively. The annealed oligonucleotides were ligated into the *Eco*RI-*Xho*I sites of pLacZi2μ (Lin et al., 2007), resulting in *HEMB1wt*:*LacZ* and *HEMB1m*:*LacZ*, respectively.

To produce a *LUC* reporter gene driven by the *HEMB1* promoter, a 1.8-kb fragment upstream of *HEMB1* ATG translational start code was PCR amplified with primers HEMB1P1 and HEMB1P2 from Col genomic DNA. The PCR fragment was inserted into the pGEM-T Easy (Promega) vector to produce pGEM-HEMB1p. To mutagenize the FBS motif (GCGCGTG) in the *HEMB1* promoter, the fragment was amplified from pGEM-HEMB1p template using primers HEMB1pm1 and HEMB1pm2 in which the FBS motif site was changed into GCttGTG, giving rise to pGEM-HEMB1pm. After sequencing confirmation, the wild-type and mutant fragments were released from pGEM-HEMB1p and pGEM-HEMB1pm cut with *Hin*dIII and *Bam*HI and ligated into the *Hin*dIII-*Bam*HI site of YY96 vector (Yamamoto et al., 1998) to produce *HEMB1p*:*LUC* and *HEMB1pm*:*LUC*, respectively.

To obtain the *HEMB1* cDNA clone, the first-strand cDNA was reverse transcripted using oligo$(dT)_{18}$ primer from total RNA extracted from Col wild-type seedlings. The ORF of *HEMB1* gene was amplified with primers HEMB1F and HEMB1R by high-fidelity *Pfu* DNA polymerase (Invitrogen) and cloned into the pGEM-T Easy vector, resulting in pGEM-HEMB1.

To construct the *HEMB1* overexpression binary vector, the *HEMB1* gene was released from pGEM-HEMB1 by digestion with *Nco*I and *Bgl*II and ligated into the *Nco*I-*Bgl*II site of pCAMBIA1302 (http://www.cambia.org/daisy/cambia/585) to produce *35S*:*HEMB1*. In addition, the *HEMB1* promoter was released from pGEM-HEMB1p cut by *Sal*I and *Sac*I and ligated into the *Sac*I-*Sal*I site of *35S*:*HEMB1* to replace the 35S promoter, resulting in *HEMB1p*:*HEMB1*.

To generate an RNAi construct for *HEMB1*, a 540-bp conserved cDNA fragment of *HEMB1* was PCR amplified with primers HEMB1R1 (containing *Spe*I and *Kpn*I sites at the 5′ end) and HEMB1R2 (containing *Sac*I and *Bam*HI sites at the 5′ end) from pGEM-HEMB1 plasmid DNA. The PCR fragment was cloned into pGEM-T Easy vector, resulting in pGEM-HEMB1R. The *Kpn*I-*Bam*HI fragment was released from pGEM-HEMB1R and ligated into the *Kpn*I-*Bam*HI site of pDS1301 (Yuan et al., 2007) to produce pDS1301-KB. Then, the *Spe*I-*Sac*I fragment was released from pGEM-HEMB1R and ligated into the *Spe*I-*Sac*I site of pDS1301-KB to produce *pDS1301-HEMB1-RNAi*.

To make the *HEMB1* amiRNA construct, the amiRNA target sequence of *HEMB1* (5′-TAACGATACTGTTTACCCCAC-3′) and primers HEMB1A1, HEMB1A2, HEMB1A3, and HEMB1A4 were designed using the WMD3 Web microRNA Designer (http://wmd3.weigelworld.org/cgi-bin/webapp.cgi; Schwab et al., 2006). These primers were used to amplify the amiRNA precursor by overlapping PCR from the pRS300 template to produce the fragment containing *HEMB1* target amiRNA foldback. The amiRNA foldback was released with *Kpn*I and *Spe*I and then ligated to the *Kpn*I-*Spe*I site of pDS1301 for constitutive expression under the control of the cauliflower mosaic virus 35S promoter, resulting in *pDS1301-HEMB1-amiRNA*.

To construct a *HEMB1* bacterial expression vector, a 1.13-kb (from amino acid 53 to 430, without the putative chloroplast transit signal peptide) cDNA fragment of *HEMB1* was PCR amplified with primers HEMB1B1 and HEMB1B2 from pGEM-HEMB1. The PCR fragment was released with *Sac*I and *Sal*I and then ligated to the *Sac*I-*Sal*I site of pET28a to produce the *pHEMB1-6His*.

To construct PIF1 bacterial expression and yeast one-hybrid vectors, the PIF1 ORF was PCR amplified with primers PIF1-F and PIF1-R from Col cDNA and cloned into pGEM-T Easy vector, resulting in pGEM-PIF1. The PCR fragment was released with *Eco*RI and *Sal*I, then ligated to the *Eco*RI-*Sal*I site of pET28a to produce *p6His-PIF1*, and ligated to the *Eco*RI-*Xho*I site of JG4-5 (Clontech) to produce GAD-PIF1, respectively.

The yeast vectors LexA-FHY3N, GAD-FHY3, and GAD-FAR1, the recombinant protein construct GST-FHY3N, and the transient expression vectors pSPYCE-FHY3 and pSPYCE-FHY3-G305R were described previously (Lin et al., 2007).

To construct LCI vectors for FHY3 and PIF1, full-length FHY3 and FHY3N were released from pGEM-FHY3 or pGEM-FHY3N by digestion with *Bam*HI and *Sal*I and cloned into the *Bam*HI-*Sal*I site of *35S*:*NLuc* (Chen et al., 2008) to produce FHY3-NLuc and FHY3N-NLuc, respectively. PIF1 was released from pGEM-PIF1 cut with *Kpn*I and *Sal*I and inserted into the *Kpn*I-*Sal*I site of *35S*:*CLuc* to generate CLuc-PIF1.

All primer sequences are listed in Supplemental Table 1 online.

Yeast Assays

Yeast hybrid assays were performed as previously described (Lin et al., 2007). Briefly, for yeast one-hybrid assays, the GAD fusion constructs were cotransformed with the *LacZ* reporter plasmids. Transformants were grown on SD/-Trp-Ura dropout liquid media, and relative β-galactosidase activity was quantified by a spectrophotometer. For yeast two-hybrid assays, the respective combinations of GAD and LexA fusions were cotransformed into the yeast strain EGY48, which contains the *LexAop*:*LacZ* reporter construct (Clontech). Transformants were grown on SD/-Trp-Ura-His dropout plates containing 5-bromo-4-chloro-3-indolyl-β-D-galactopyranoside for blue color development.

Purification of Recombinant Protein

GST, GST-FHY3N, His-PIF1, and His-HEMB1 recombinant fusion proteins were induced by isopropyl β-D-1-thiogalactopyranoside and expressed in the *Escherichia coli* BL21 (DE3) strain. The proteins were then purified by Glutathione Sepharose 4B beads (GE Healthcare; for GST and GST-FHY3N) or Ni-NTA Agarose (Qiagen; for His-PIF1 and His-HEMB1) following the manufacturer's instructions.

EMSA

EMSA analysis was performed as previously described (Lin et al., 2007). Briefly, *HEMB1* complementary oligonucleotides were labeled with [α-^{32}P]dATP and incubated with GST-FHY3N or GST proteins in the absence or presence of unlabeled oligonucleotides followed by separation on polyacrylamide gels. The DNA–protein binding signal was exposed to x-ray film and developed. The oligonucleotide sequences are shown in Supplemental Table 1 online.

Antibody Production and Immunoblotting

The peptide corresponding to amino acids 336 to 346 of ALAD (EAREDEAEGAD) conjugated with KLH was synthesized (Cali-Bio), and polyclonal antibody was raised in rabbit. For immunoblotting, seedlings were homogenized in extraction buffer containing 50 mM Tris-HCl, pH 7.5, 150 mM NaCl, 10 mM $MgCl_2$, 0.1% Tween 20, 1 mM PMSF, and 1

complete protease inhibitor cocktail (Roche). The extracts were centrifuged at 14,000*g* twice at 4°C for 10 min each, and protein concentration was determined by Bradford assay (Bio-Rad). Proteins were boiled in SDS loading buffer, separated by 10% SDS-PAGE gels, and blotted onto polyvinylidene fluoride membranes (Pall). The proteins were then incubated with anti-ALAD (1:1000 dilution) or anti-His (Abcam) primary antibodies and subsequently the horseradish peroxidase–conjugated goat-anti-rabbit secondary antibody (Abcam). The protein bands were visualized by the standard ECL method.

Pull-Down Assay

About 2 μg of purified recombinant bait proteins (GST-FHY3N and GST) and 2 μg of prey proteins (His-PIF1) were incubated in binding buffer (50 mM Tris-HCl, pH 7.5, 100 mM NaCl, and 0.6% Triton X-100) for 2 h at 4°C. Glutathione Sepharose 4B beads were added and incubated for 1 h. After washing with binding buffer, precipitated proteins were eluted in 2× SDS loading buffer. The proteins were then size fractioned on 10% SDS-PAGE and immunoblotted by anti-His or anti-GST antibodies (Abcam).

Coimmunoprecipitation

For coimmunoprecipitation assays, seedlings were grown in the dark followed by treatment with 50 μM MG132. Total proteins were extracted with extraction buffer and incubated with 2 μg anti-GUS (Invitrogen) antibody for 2 to 3 h at 4°C. Fifty microliters of protein G-Sepharose (Roche) was added and incubated for another 2 to 3 h. The sepharose beads were washed three times with coimmumoprecipitation buffer, and the precipitated proteins were eluted in 2× SDS loading buffer by boiling for 10 min. The proteins were separated on 10% SDS-PAGE gel and detected by immunoblotting using anti-MYC (Abcam) and anti-GUS antibodies.

ChIP

The *35S*:*GUS-FHY3* transgenic plants grown in darkness for 5 d were used for ChIP assays following the procedure as described (Leibfried et al., 2005). Briefly, the seedlings were cross-linked with 1% formaldehyde and ground to powder under liquid nitrogen. After isolation and sonication, the chromatin complexes were incubated with anti-GUS antibody (Invitrogen) or anti-FLAG antibody (Abcam) as a negative control. The precipitated DNA fragments were recovered and quantified by real-time PCR with primers shown in Supplemental Table 1 online.

LUC Activity Assay

Protoplast isolation and transient expression assays were performed as described previously (Lin et al., 2007). For transient expression assays, the reporter plasmids (*HEMB1p*:*LUC* or *HEMB1pm*:*LUC*), effector constructs (*pSPYCE-FHY3* and *pSPYCE-FHY3-G305R*), and *35S*:*GUS* internal control were cotransformed into protoplasts. For LCI assays, plastid combinations of various N- and C-terminal LUC fusions were cotransformed with *35S*:*GUS* internal control. The protoplasts were pelleted and resuspended in 1× cell culture lysis reagent (Promega). The GUS fluorescence was measured using a Modulus luminometer/fluorometer with a UV fluorescence optical kit (Promega). The LUC activity was detected with a luminescence kit using LUC assay substrate (Promega). The relative reporter gene expression levels were expressed as the LUC/GUS ratios.

RNA Extraction and qRT-PCR

Seedlings were treated as indicated in the text, and plant total RNA was extracted by RNA extraction kit (Tiangen). The first-strand cDNA was synthesized by reverse transcriptase (Invitrogen). Real-time PCR was performed with the SYBR Premix ExTaq kit (Takara) in a 15-μL reaction system following the manufacturer's instructions. Three biological replicates were performed for each sample, and the expression levels were normalized to those of *UBQ*. All primers sequences are listed in Supplemental Table 1 online.

In Vivo ALA Feeding

For phenotype analysis, the seedlings were grown on MS plates containing 100 μM ALA (Sigma-Aldrich) in darkness for 4 d. For ALAD activity assay, the dark-grown seedlings were transferred to 10 mM ALA solution (5 mM $MgCl_2$ and 10 mM NaH_2PO_4, pH 7.0) under green light and incubated for 12 h.

ALAD Enzyme Activity Determination and PBG Measurement

The in vitro ALAD activity was determined as Vajpayee et al. (2000) described with minor modifications. Briefly, tissues (~0.2 g) were homogenized with 1 mL extraction buffer (50 mM Tris-HCl, pH 8.2, and 0.1 mM DTT) in a prechilled mortar and pestle. The homogenate was filtered through four layers of cheese cloth, and the filtrate was centrifuged at 10,000*g* for 1 h at 4°C. The supernatant was used for ALAD activity assay. One milliliter of the extract was incubated with reaction buffer (0.27 mL of 1 mg/mL ALA, 1.35 mL of 50 mM Tris-HCl, pH 8.2, 0.1 mM DTT, and 0.08 mL of 0.2 M $MgCl_2$) for 2.5 h at 37°C. The reaction was terminated by the addition of 0.3 mL of 3.0 M trichloroacetic acid. After cooling, samples were centrifuged at 2000*g* for 10 min and used for PBG determination. The ALAD activity is expressed as nmol of PBG formed/mg protein/h at 37°C.

PBG content determination was performed as described (Mauzerall and Granick, 1956; Kayser et al., 2005). Briefly, samples were homogenized and resuspended in 1 mL of 0.15 M cold trichloroacetic acid. After centrifugation at 50,000*g* for 30 min at 0°C, the supernatants were adjusted to a pH of ~5.5 by addition of 1 N NaOH and 0.5 M sodium acetate. They were passed through a Dowex 1×8 column (200 to 400 mesh; Sigma-Aldrich) equilibrated at pH 4.6 to absorb PBG. The resins were washed eight times with double distilled water, and PBG was eluted two times with 0.4 mL of 1 M acetic acid. The eluates were mixed with an equal volume of Ehrlich reagent, and absorbance of the mixture was determined at 555 nm after 10 min on a spectrophotometer. PBG content of the samples was calculated using a standard curve generated by commercial PBG (Sigma-Aldrich).

Heme Determination

The content of noncovalently bound heme was measured according to the method of Richter et al. (2010). Briefly, tissues were homogenized, and noncovalently bound heme was extracted with 5 mL of extraction solution (2 mL of dimethyl sulfoxide, 10 mL of acetone, and 0.5 mL of 37% HCl) followed by centrifugation at 16,000*g* for 10 min. Heme was transferred to ether by addition of 3 mL of diethyl ether, 2 mL of saturated NaCl, and 10 mL of water. The ether phase was mixed with ethanol and flowed through a DEAE-Sepharose CL-6B column (GE Healthcare). After sequential washing with diethyl ether:ethanol (3:1, v/v), diethyl ether:ethanol (1:1, v/v), and ethanol, heme was eluted with ethanol:acetic acid:water (81:9:10, v/v/v) and quantified spectrophotometrically at 398 nm using the extinction coefficient of 144 mM^{-1} cm^{-1}.

Arabidopsis Transformation

The plant binary expression vectors *35S*:*HEMB1*, *HEMB1p*:*HEMB1*, *pDS1301-HEMB1-RNAi*, or *pDS1301-HEMB1-amiRNA* were electroporated into the *Agrobacterium tumefaciens* strain GV3101 and then introduced into the wild type or *fhy3 far1* via the floral dip method (Clough and Bent, 1998). Transgenic plants were selected on MS plates in the presence of 50 mg/L hygromycin.

Accession Numbers

Sequence data from this article can be found in the Arabidopsis Genome Initiative or GenBank/EMBL data libraries under the following accession numbers: *FHY3* (At3g22170), *FAR1* (At4g15090), *HEMB1* (At1g69740), *PIF1* (At2g20180), *UBQ* (At3g52590), *HEMA1* (At1g58290), *HEMA2* (At1g09940), *HEMA3* (At2g31250), *GSA1* (At5g63570), *GSA2* (At3g48730), *HEMB2* (At1g44318), *HEMC* (At5g08280), *HEMD* (At2g26540), *HEME1* (At3g14930), *HEME2* (At2g40490), *HEMF1* (At1g03475), *HEMF2* (At4g03205), *CPO3* (At5g63290), *HEMG1* (At4g01690), *HEMG2* (At5g14220), *FC1* (At5g26030), *FC2* (At2g30390), *HO1* (At2g26670), *HO2* (At2g26550), *HO3* (At1g69720), *HO4* (At1g58300), *HY2* (At3g09150), *CHLD* (At1g08520), *CHLH* (At5g13630), *CHLI1* (At4g18480), *CHLI2* (At5g45930), *CHLM* (At4g25080), *CRD1* (At3g56940), *PORA* (At5g54190), *PORB* (At4g27440), *PORC* (At1g03630), *DVR* (AT5G18660), *CAO* (At1g44446), and *CHLG* (At3g51820).

Supplemental Data

The following materials are available in the online version of this article.

Supplemental Figure 1. Relative Pchlide Fluorescence of Various Mutants and the Wild Type.

Supplemental Figure 2. Noncovalently Bound Heme Contents in *fhy3*, *far1*, and *fhy3 far1* Mutants and the Wild Type.

Supplemental Figure 3. Expression of Genes Involved in the Tetrapyrrole Biosynthetic Pathway.

Supplemental Figure 4. Confirmation of ALAD Antibody and Protein Level.

Supplemental Figure 5. *HEMB1* and *HEMB2* Expression Patterns in Different Stages and Tissues.

Supplemental Figure 6. Phenotype of *HEMB1* Overexpression Plants.

Supplemental Figure 7. Identification and Characterization of *hemb1* Mutant.

Supplemental Figure 8. Interaction between FHY3 and PIF1.

Supplemental Figure 9. *FHY3* and *HEMB1* Are Induced by Light.

Supplemental Figure 10. Characterization of the *arc5* Mutant Phenotype.

Supplemental Table 1. List of Primers Used in This Study.

ACKNOWLEDGMENTS

We thank Hongwei Guo for his valuable comments on this article. We also thank Tingyun Kuang, Lixin Zhang, and Congming Lu for stimulating discussions. We thank Enamul Huq for providing *pif1-2* seeds, Xing Wang Deng for providing *arc5* seeds, Shiping Wang for providing pDS1301 vector, and the ABRC for providing T-DNA seeds. This work was supported by grants from the Chinese Academy of Sciences, the National Natural Science Foundation of China (30970254 and 31170221), the Ministry of Agriculture of China (2011ZX08009-003), and the State Basic Research Development Program (2009CB118500) to R.L.

AUTHOR CONTRIBUTIONS

W.T. and R.L. designed research. W.T., W.W., Q.J., D.C., and Y.J performed research. W.T., W.W., H.W., and R.L. analyzed data. R.L. wrote the article.

Received February 14, 2012; revised April 30, 2012; accepted May 10, 2012; published May 25, 2012.

REFERENCES

Adhikari, N.D., Froehlich, J.E., Strand, D.D., Buck, S.M., Kramer, D.M., and Larkin, R.M. (2011). GUN4-porphyrin complexes bind the ChlH/GUN5 subunit of Mg-Chelatase and promote chlorophyll biosynthesis in *Arabidopsis*. Plant Cell **23:** 1449–1467.

Allen, T., Koustenis, A., Theodorou, G., Somers, D.E., Kay, S.A., Whitelam, G.C., and Devlin, P.F. (2006). *Arabidopsis* FHY3 specifically gates phytochrome signaling to the circadian clock. Plant Cell **18:** 2506–2516.

Al-Sady, B., Ni, W., Kircher, S., Schäfer, E., and Quail, P.H. (2006). Photoactivated phytochrome induces rapid PIF3 phosphorylation prior to proteasome-mediated degradation. Mol. Cell **23:** 439–446.

Battersby, A.R. (2000). Tetrapyrroles: The pigments of life. Nat. Prod. Rep. **17:** 507–526.

Bryant, N., Lloyd, J., Sweeney, C., Myouga, F., and Meinke, D. (2011). Identification of nuclear genes encoding chloroplast-localized proteins required for embryo development in Arabidopsis. Plant Physiol. **155:** 1678–1689.

Buhr, F., El Bakkouri, M., Valdez, O., Pollmann, S., Lebedev, N., Reinbothe, S., and Reinbothe, C. (2008). Photoprotective role of NADPH:protochlorophyllide oxidoreductase A. Proc. Natl. Acad. Sci. USA **105:** 12629–12634.

Casal, J.J., Fankhauser, C., Coupland, G., and Blázquez, M.A. (2004). Signalling for developmental plasticity. Trends Plant Sci. **9:** 309–314.

Cheminant, S., Wild, M., Bouvier, F., Pelletier, S., Renou, J.P., Erhardt, M., Hayes, S., Terry, M.J., Genschik, P., and Achard, P. (2011). DELLAs regulate chlorophyll and carotenoid biosynthesis to prevent photooxidative damage during seedling deetiolation in *Arabidopsis*. Plant Cell **23:** 1849–1860.

Chen, H.M., Zou, Y., Shang, Y.L., Lin, H.Q., Wang, Y.J., Cai, R., Tang, X.Y., and Zhou, J.M. (2008). Firefly luciferase complementation imaging assay for protein-protein interactions in plants. Plant Physiol. **146:** 368–376.

Clough, S.J., and Bent, A.F. (1998). Floral dip: A simplified method for Agrobacterium-mediated transformation of *Arabidopsis thaliana*. Plant J. **16:** 735–743.

Czarnecki, O., Hedtke, B., Melzer, M., Rothbart, M., Richter, A., Schröter, Y., Pfannschmidt, T., and Grimm, B. (2011). An *Arabidopsis* GluTR binding protein mediates spatial separation of 5-aminolevulinic acid synthesis in chloroplasts. Plant Cell **23:** 4476–4491.

Eckhardt, U., Grimm, B., and Hörtensteiner, S. (2004). Recent advances in chlorophyll biosynthesis and breakdown in higher plants. Plant Mol. Biol. **56:** 1–14.

Goslings, D., Meskauskiene, R., Kim, C., Lee, K.P., Nater, M., and Apel, K. (2004). Concurrent interactions of heme and FLU with Glu tRNA reductase (HEMA1), the target of metabolic feedback inhibition of tetrapyrrole biosynthesis, in dark- and light-grown *Arabidopsis* plants. Plant J. **40:** 957–967.

Herr, J.M. Jr. (1971). A new clearing squash technique for the study of ovule development in angiosperms. Am. J. Bot. **58:** 785–790.

Heyes, D.J., and Hunter, C.N. (2005). Making light work of enzyme catalysis: Protochlorophyllide oxidoreductase. Trends Biochem. Sci. **30:** 642–649.

Hsu, S.-C., Belmonte, M.F., Harada, J.J., and Inoue, K. (2010). Indispensable roles of plastids in *Arabidopsis thaliana* embryogenesis. Curr. Genomics **11:** 338–349.

Hudson, M., Ringli, C., Boylan, M.T., and Quail, P.H. (1999). The FAR1 locus encodes a novel nuclear protein specific to phytochrome A signaling. Genes Dev. **13:** 2017–2027.

Hudson, M.E., Lisch, D.R., and Quail, P.H. (2003). The *FHY3* and *FAR1* genes encode transposase-related proteins involved in regulation of gene expression by the phytochrome A-signaling pathway. Plant J. **34:** 453–471.

Huq, E., Al-Sady, B., Hudson, M., Kim, C., Apel, K., and Quail, P.H. (2004). Phytochrome-interacting factor 1 is a critical bHLH regulator of chlorophyll biosynthesis. Science **305:** 1937–1941.

Jiao, Y., Lau, O.S., and Deng, X.W. (2007). Light-regulated transcriptional networks in higher plants. Nat. Rev. Genet. **8:** 217–230.

Joo, J.H., Wang, S.Y., Chen, J.G., Jones, A.M., and Fedoroff, N.V. (2005). Different signaling and cell death roles of heterotrimeric G protein α and β subunits in the *Arabidopsis* oxidative stress response to ozone. Plant Cell **17:** 957–970.

Kaczor, C.M., Smith, M.W., Sangwan, I., and O'Brian, M.R. (1994). Plant δ-aminolevulinic acid dehydratase. Expression in soybean root nodules and evidence for a bacterial lineage of the *Alad* gene. Plant Physiol. **104:** 1411–1417.

Kayser, H., Krull-Savage, U., and Rilk-van Gessel, R. (2005). Developmental profiles of 5-aminolevulinate, porphobilinogen and porphobilinogen synthase activity in *Pieris brassicae* related to the synthesis of the bilin-binding protein. Insect Biochem. Mol. Biol. **35:** 165–174.

Kim, J., Yi, H., Choi, G., Shin, B., Song, P.-S., and Choi, G. (2003). Functional characterization of phytochrome interacting factor 3 in phytochrome-mediated light signal transduction. Plant Cell **15:** 2399–2407.

Kleine, T., Kindgren, P., Benedict, C., Hendrickson, L., and Strand, Å. (2007). Genome-wide gene expression analysis reveals a critical role for CRYPTOCHROME1 in the response of Arabidopsis to high irradiance. Plant Physiol. **144:** 1391–1406.

Kumar, A.M., and Söll, D. (2000). Antisense *HEMA1* RNA expression inhibits heme and chlorophyll biosynthesis in Arabidopsis. Plant Physiol. **122:** 49–56.

Larkin, R.M., Alonso, J.M., Ecker, J.R., and Chory, J. (2003). GUN4, a regulator of chlorophyll synthesis and intracellular signaling. Science **299:** 902–906.

Leibfried, A., To, J.P.C., Busch, W., Stehling, S., Kehle, A., Demar, M., Kieber, J.J., and Lohmann, J.U. (2005). WUSCHEL controls meristem function by direct regulation of cytokinin-inducible response regulators. Nature **438:** 1172–1175.

Leivar, P., and Quail, P.H. (2011). PIFs: Pivotal components in a cellular signaling hub. Trends Plant Sci. **16:** 19–28.

Leivar, P., Tepperman, J.M., Monte, E., Calderon, R.H., Liu, T.L., and Quail, P.H. (2009). Definition of early transcriptional circuitry involved in light-induced reversal of PIF-imposed repression of photomorphogenesis in young *Arabidopsis* seedlings. Plant Cell **21:** 3535–3553.

Li, G. et al. (2011). Coordinated transcriptional regulation underlying the circadian clock in *Arabidopsis*. Nat. Cell Biol. **13:** 616–622.

Li, J., Li, G., Gao, S., Martinez, C., He, G., Zhou, Z., Huang, X., Lee, J.-H., Zhang, H., Shen, Y., Wang, H., and Deng, X.W. (2010). *Arabidopsis* transcription factor ELONGATED HYPOCOTYL5 plays a role in the feedback regulation of phytochrome A signaling. Plant Cell **22:** 3634–3649.

Lin, C. (2002). Blue light receptors and signal transduction. Plant Cell **14 (suppl.):** S207–S225.

Lin, R., Ding, L., Casola, C., Ripoll, D.R., Feschotte, C., and Wang, H. (2007). Transposase-derived transcription factors regulate light signaling in *Arabidopsis*. Science **318:** 1302–1305.

Lin, R., Teng, Y., Park, H.-J., Ding, L., Black, C., Fang, P., and Wang, H. (2008). Discrete and essential roles of the multiple domains of Arabidopsis FHY3 in mediating phytochrome A signal transduction. Plant Physiol. **148:** 981–992.

Maruno, M. et al. (2001). Highly heterogeneous nature of δ-aminolevulinate dehydratase (ALAD) deficiencies in ALAD porphyria. Blood **97:** 2972–2978.

Matsumoto, F., Obayashi, T., Sasaki-Sekimoto, Y., Ohta, H., Takamiya, K., and Masuda, T. (2004). Gene expression profiling of the tetrapyrrole metabolic pathway in Arabidopsis with a mini-array system. Plant Physiol. **135:** 2379–2391.

Mauzerall, D., and Granick, S. (1956). The occurrence and determination of δ-amino-levulinic acid and porphobilinogen in urine. J. Biol. Chem. **219:** 435–446.

Meskauskiene, R., Nater, M., Goslings, D., Kessler, F., op den Camp, R., and Apel, K. (2001). FLU: A negative regulator of chlorophyll biosynthesis in *Arabidopsis thaliana*. Proc. Natl. Acad. Sci. USA **98:** 12826–12831.

Mochizuki, N., Brusslan, J.A., Larkin, R., Nagatani, A., and Chory, J. (2001). *Arabidopsis genomes uncoupled 5* (*GUN5*) mutant reveals the involvement of Mg-chelatase H subunit in plastid-to-nucleus signal transduction. Proc. Natl. Acad. Sci. USA **98:** 2053–2058.

Mochizuki, N., Tanaka, R., Grimm, B., Masuda, T., Moulin, M., Smith, A.G., Tanaka, A., and Terry, M.J. (2010). The cell biology of tetrapyrroles: A life and death struggle. Trends Plant Sci. **15:** 488–498.

Monte, E., Tepperman, J.M., Al-Sady, B., Kaczorowski, K.A., Alonso, J.M., Ecker, J.R., Li, X., Zhang, Y.L., and Quail, P.H. (2004). The phytochrome-interacting transcription factor, PIF3, acts early, selectively, and positively in light-induced chloroplast development. Proc. Natl. Acad. Sci. USA **101:** 16091–16098.

Moon, J., Zhu, L., Shen, H., and Huq, E. (2008). PIF1 directly and indirectly regulates chlorophyll biosynthesis to optimize the greening process in *Arabidopsis*. Proc. Natl. Acad. Sci. USA **105:** 9433–9438.

Neff, M.M., Fankhauser, C., and Chory, J. (2000). Light: An indicator of time and place. Genes Dev. **14:** 257–271.

op den Camp, R.G.L., Przybyla, D., Ochsenbein, C., Laloi, C., Kim, C., Danon, A., Wagner, D., Hideg, É., Göbel, C., Feussner, I., Nater, M., and Apel, K. (2003). Rapid induction of distinct stress responses after the release of singlet oxygen in *Arabidopsis*. Plant Cell **15:** 2320–2332.

Ouyang, X. et al. (2011). Genome-wide binding site analysis of FAR-RED ELONGATED HYPOCOTYL3 reveals its novel function in *Arabidopsis* development. Plant Cell **23:** 2514–2535.

Oyama, T., Shimura, Y., and Okada, K. (1997). The *Arabidopsis HY5* gene encodes a bZIP protein that regulates stimulus-induced development of root and hypocotyl. Genes Dev. **11:** 2983–2995.

Peter, E., and Grimm, B. (2009). GUN4 is required for post-translational control of plant tetrapyrrole biosynthesis. Mol. Plant **2:** 1198–1210.

Polking, G.F., Hannapel, D.J., and Gladon, R.J. (1995). A cDNA clone for 5-aminolevulinic acid dehydratase from tomato (*Lycopersicon esculentum* Mill.). Plant Physiol. **107:** 1033–1034.

Reinbothe, S., Reinbothe, C., Apel, K., and Lebedev, N. (1996). Evolution of chlorophyll biosynthesis—The challenge to survive photooxidation. Cell **86:** 703–705.

Richter, A., Peter, E., Pörs, Y., Lorenzen, S., Grimm, B., and Czarnecki, O. (2010). Rapid dark repression of 5-aminolevulinic acid synthesis in green barley leaves. Plant Cell Physiol. **51:** 670–681.

Runge, S., Sperling, U., Frick, G., Apel, K., and Armstrong, G.A. (1996). Distinct roles for light-dependent NADPH:protochlorophyllide oxidoreductases (POR) A and B during greening in higher plants. Plant J. **9:** 513–523.

Schmied, J., Hedtke, B., and Grimm, B. (2011). Overexpression of *HEMA1* encoding glutamyl-tRNA reductase. J. Plant Physiol. **168:** 1372–1379.

Schubert, H.L., Erskine, P.T., and Cooper, J.B. (2009). 5-Aminolaevulinic acid dehydratase, porphobilinogen deaminase and uroporphyrinogen III synthase. In Tetrapyrroles: Birth, Life and Death, M.J. Warren and A.G. Smith, eds (Austin, TX: Landes Bioscience and Springer Science and Business Media), pp. 43–73.

Schulze, A., Frommhold, D., Hoffmann, G.F., and Mayatepek, E. (2001). Spectrophotometric microassay for δ-aminolevulinate dehydratase in dried-blood spots as confirmation for hereditary tyrosinemia type I. Clin. Chem. **47:** 1424–1429.

Schwab, R., Ossowski, S., Riester, M., Warthmann, N., and Weigel, D. (2006). Highly specific gene silencing by artificial microRNAs in *Arabidopsis*. Plant Cell **18:** 1121–1133.

Shen, H., Moon, J., and Huq, E. (2005). PIF1 is regulated by light-mediated degradation through the ubiquitin-26S proteasome pathway to optimize photomorphogenesis of seedlings in *Arabidopsis*. Plant J. **44:** 1023–1035.

Shin, J., Kim, K., Kang, H.J., Zulfugarov, I.S., Bae, G., Lee, C.H., Lee, D., and Choi, G. (2009). Phytochromes promote seedling light responses by inhibiting four negatively-acting phytochrome-interacting factors. Proc. Natl. Acad. Sci. USA **106:** 7660–7665.

Solymosi, K., and Schoefs, B. (2010). Etioplast and etio-chloroplast formation under natural conditions: The dark side of chlorophyll biosynthesis in angiosperms. Photosynth. Res. **105:** 143–166.

Sperling, U., van Cleve, B., Frick, G., Apel, K., and Armstrong, G.A. (1997). Overexpression of light-dependent PORA or PORB in plants depleted of endogenous POR by far-red light enhances seedling survival in white light and protects against photooxidative damage. Plant J. **12:** 649–658.

Stephenson, P.G., Fankhauser, C., and Terry, M.J. (2009). PIF3 is a repressor of chloroplast development. Proc. Natl. Acad. Sci. USA **106:** 7654–7659.

Stephenson, P.G., and Terry, M.J. (2008). Light signalling pathways regulating the Mg-chelatase branchpoint of chlorophyll synthesis during de-etiolation in *Arabidopsis thaliana*. Photochem. Photobiol. Sci. **7:** 1243–1252.

Su, Q., Frick, G., Armstrong, G., and Apel, K. (2001). POR C of *Arabidopsis thaliana*: A third light- and NADPH-dependent protochlorophyllide oxidoreductase that is differentially regulated by light. Plant Mol. Biol. **47:** 805–813.

Tanaka, R., and Tanaka, A. (2007). Tetrapyrrole biosynthesis in higher plants. Annu. Rev. Plant Biol. **58:** 321–346.

Tanaka, A., and Tanaka, R. (2006). Chlorophyll metabolism. Curr. Opin. Plant Biol. **9:** 248–255.

Vajpayee, P., Tripathi, R.D., Rai, U.N., Ali, M.B., and Singh, S.N. (2000). Chromium (VI) accumulation reduces chlorophyll biosynthesis, nitrate reductase activity and protein content in *Nymphaea alba* L. Chemosphere **41:** 1075–1082.

Von Arnim, A., and Deng, X.W. (1996). Light control of seedling development. Annu. Rev. Plant Physiol. Plant Mol. Biol. **47:** 215–243.

Wagner, D., Przybyla, D., Op den Camp, R., Kim, C., Landgraf, F., Lee, K.P., Würsch, M., Laloi, C., Nater, M., Hideg, E., and Apel, K. (2004). The genetic basis of singlet oxygen-induced stress responses of *Arabidopsis thaliana*. Science **306:** 1183–1185.

Wang, H., and Deng, X.W. (2002). *Arabidopsis* FHY3 defines a key phytochrome A signaling component directly interacting with its homologous partner FAR1. EMBO J. **21:** 1339–1349.

Wang, H., Ma, L., Habashi, J., Li, J.M., Zhao, H.Y., and Deng, X.W. (2002). Analysis of far-red light-regulated genome expression profiles of phytochrome A pathway mutants in *Arabidopsis*. Plant J. **32:** 723–733.

Whitelam, G.C., Johnson, E., Peng, J., Carol, P., Anderson, M.L., Cowl, J.S., and Harberd, N.P. (1993). Phytochrome A null mutants of *Arabidopsis* display a wild-type phenotype in white light. Plant Cell **5:** 757–768.

Yamamoto, Y.Y., Matsui, M., Ang, L.-H., and Deng, X.W. (1998). Role of a COP1 interactive protein in mediating light-regulated gene expression in *Arabidopsis*. Plant Cell **10:** 1083–1094.

Yang, J., Lin, R., Sullivan, J., Hoecker, U., Liu, B., Xu, L., Deng, X. W., and Wang, H. (2005). Light regulates COP1-mediated degradation of HFR1, a transcription factor essential for light signaling in *Arabidopsis*. Plant Cell **17:** 804–821.

Yuan, B., Shen, X., Li, X., Xu, C., and Wang, S. (2007). Mitogen-activated protein kinase OsMPK6 negatively regulates rice disease resistance to bacterial pathogens. Planta **226:** 953–960.

Zhong, S.W., Zhao, M.T., Shi, T.Y., Shi, H., An, F.Y., Zhao, Q., and Guo, H.W. (2009). EIN3/EIL1 cooperate with PIF1 to prevent photo-oxidation and to promote greening of *Arabidopsis* seedlings. Proc. Natl. Acad. Sci. USA **106:** 21431–21436.